Can liquid-liquid equilibria be predicted by the combination of a cubic equation of state and a g E model not suitable for liquid-liquid equilibria?

Romain Privat, Jean-Noël Jaubert, Georgios Kontogeorgis

Fluid Phase Equilibria 589 (2025) 114249

Contents lists available at ScienceDirect

Fluid Phase Equilibria

journal homepage: www.journals.elsevier.com/fluid-phase-equilibria

Can liquid-liquid equilibria be predicted by the combination of a cubic equation of state and a g^E model not suitable for liquid-liquid equilibria?

Romain Privat [a,*], Jean-Noël Jaubert [a,*], Georgios M. Kontogeorgis [b,*]

[a] Université de Lorraine, CNRS, LRGP, F-54000, Nancy, France
[b] Center for Energy Resources Engineering (CERE), Department of Chemical and Biochemical Engineering, Building 229, Technical University of Denmark, Denmark

ARTICLE INFO

Keywords:
Mixing rules
Huron-Vidal
MHV1
Wilson
Zero reference pressure

ABSTRACT

In modern versions of cubic equations of state (EoS), the mixing rules for EoS parameters are derived from an activity coefficient model using either the Huron-Vidal or the Zero Reference Pressure (ZRP) approach. As it is a fact that Wilson's activity coefficient model cannot predict liquid-liquid equilibria (LLE), this article attempts to answer the question: if Wilson's model is coupled with a cubic EoS, is the resulting model capable of predicting LLE?

This question is actually becoming increasingly important as recent EoS rely on such a coupling (e.g., the tc-PR EoS). We show that although Wilson's model is mathematically unable to predict instable liquid phases, this is not true for Wilson-EoS models (i.e., EoS incorporating Wilson's model). However, it is also shown that the capacity of Wilson-EoS to predict LLE depends not only on the approach chosen (Huron-Vidal or ZRP) but also on mixture characteristics (such as the ratio of covolumes, the ratio of critical attractive parameters, the binary interaction parameters etc.).

1. Introduction

Cubic Equations of State (CEoS) are certainly among the most widely used thermodynamic models for the design and simulation of chemical engineering processes. *What is the reason for this success?* It is undoubtedly due to their ability to correlate or predict most of the fluid-phase equilibria, to allow the estimation of energetic properties (enthalpy, entropy, exergy, heat capacity etc.) as well as the possibility to use them in extrapolation, all this with a reasonable accuracy and a limited number of parameters. However, this class of models also has some shortcomings. While it is generally accepted that they provide accurate representation of mixtures containing low-polarity compounds, the representation of mixtures containing highly polar and associating compounds is often considered to be unsatisfactory when Van der Waals 1-fluid mixing and combining rules are used.

One of the most common way to boost the cubic models and improve the description of polar / associating mixtures lies in their hybridization with activity-coefficient (AC) models, also called excess Gibbs energy (g^E) models. Overall, AC models show good performance when CEoS are likely to fail and, conversely, moderate performance when CEoS perform well:

- Although the CEoS model has the ability to represent the entire phase space of a fluid, covering a range from low to high pressure and temperature, including sub- and super-critical domains, AC models are limited to the low-pressure subcritical regions where no vapor-liquid critical phenomenon can occur,
- However, AC models can describe associating and polar mixtures with accuracy where CEoS cannot.

The idea of combining AC models and CEoS arose from the realization that this could lead to a new type of model that shows the best features of both CEoS and AC models alone. To achieve this fusion, Huron and Vidal introduced the so-called "EoS/g^E mixing rules". The basic idea is to equate the g^E expressions obtained from the CEoS (denoted g^E_{EoS}) and from the AC model (denoted $g^{E,\gamma}$) in order to get an expression of the ratio $\frac{a}{RTb}$, where a and b are the classical attractive term coefficient and covolume of the CEoS. The parameter $\frac{a}{RTb}$ is involved in the expression of g^E_{EoS}. By assuming a given mixing rule for the b parameter (linear or quadratic, generally), the mixing rule for parameter a can be obtained from the $\frac{a}{RTb}$ expression.

Since CEoS do not assume that liquid properties are pressure independent, while AC models do, the g^E_{EoS} expression depends on three

* Corresponding authors.
E-mail addresses: romain.privat@univ-lorraine.fr (R. Privat), jean-noel.jaubert@univ-lorraine.fr (J.-N. Jaubert), gk@kt.dtu.dk (G.M. Kontogeorgis).

https://doi.org/10.1016/j.fluid.2024.114249
Received 30 July 2024; Received in revised form 2 October 2024; Accepted 7 October 2024
Available online 12 October 2024

variables - temperature, pressure, and composition - while the $g^{E,\gamma}$ expression depends on two variables only, the temperature and the composition. This is the reason why a reference pressure P_{ref} is used for equating both g^E expressions.

$$g^E_{EoS}\left(T, P_{ref}, \boldsymbol{x}, \frac{a}{RTb}\right) = g^{E,\gamma}(T, \boldsymbol{x}) \quad (1)$$

Eq. (1) is hereafter referred to as the *matching* equation and can be solved at specified $(T, \boldsymbol{x}, P_{ref})$ to get an expression for $\frac{a}{RTb}$.

Huron and Vidal proposed to use $P_{ref} = +\infty$ [1] while, some years after, Mollerup [2] and Michelsen [3,4] used $P_{ref} = 0$, thus giving birth to the two major families of CEoS mixing rules called Huron-Vidal and zero reference pressure, ZRP (sometimes called "Michelsen approach" [5]), respectively. Their detailed expressions are introduced in Section 2. Note that the general formulation of the ZRP mixing rule can only be applied at low temperature, i.e., on a domain where the CEoS can predict liquid-like roots. This approach is called exact ZRP mixing rule. To overpass this important limitation, approximate ZRP mixing rules, namely the MHV1 and MHV2 versions, applicable at any temperature without restriction, were proposed by Michelsen [3] and Dahl et al. [6,7], respectively. These mixing rules are said "approximate" because they induce an approximate zero reference pressure ($P_{ref} \approx 0$). In other terms, there is not a strict equality between g^E_{EoS} and $g^{E,\gamma}$ at $P = 0$ when using MHV1 or MHV2.

Various AC models were incorporated within EoS/g^E mixing rules (i.e., HV, MHV1, MHV2) and in particular, the NRTL, Van Laar, UNIQUAC and UNIFAC $g^{E,\gamma}$ models were extensively used.

- In their seminal article, Huron and Vidal combined the NRTL AC model with the Soave-Redlich-Kwong (SRK) EoS [1]. Other authors considered the UNIQUAC model or its predictive version, the UNIFAC model [8–14]. Note that the predictive PPR78 and *E*-PPR78 CEoS were built by associating a predictive form of the Van Laar AC model and the 1978 version of the Peng-Robinson (PR) EoS through HV mixing rules [15–18].
- In the papers [3,4] introducing the ZRP mixing rules, Michelsen opted for a singular combination: he associated the SRK CEoS and the Wilson AC model through the MHV1 mixing rules and illustrated the performance of the proposed approach on the zeotropic acetone + water system and the azeotropic ethanol + water and methanol + benzene systems, all at atmospheric pressure. In relation with the question asked in the title of the present study, let us point out that none of these systems show liquid-liquid phase separation.

  The popularity of the ZRP mixing rule has increased considerably thanks to the PSRK model, a version of the SRK EoS proposed by Gmehling et al. [19–23] that was made predictive by combining the predictive $g^{E,\gamma}$ model UNIFAC with a MHV1 type mixing rule.
  Some authors developed also predictive EoS based on the MHV2 mixing rule and the UNIFAC model [6,7].

At the noticeable exception of both Michelsen's articles introducing the ZRP approach, the possibility to incorporate the Wilson AC model in a CEoS through EoS/g^E mixing rules seems to be ignored by model developers. Why has this AC model not been considered while it is acknowledged for its good capacity to model complex mixtures at low pressure?

In our opinion, the main reason is its well-documented inability to predict liquid-liquid phase equilibria (LLE) which is suspected to persist when the model is incorporated in a CEoS.

As related in a recent paper [24] about the Wilson AC model, at a recent conference, some of the authors of this manuscript presented the results of liquid-liquid equilibrium (LLE) calculations performed with the *tc*-PR-Wilson EoS [25–28] - that is the translated [29,30] and consistent Peng-Robinson EoS combined with the residual part of the Wilson model [28]. A colleague, well-known thermodynamicist, was puzzled and asked a question: "*But the Wilson equation does not give LLE! How is then possible to get LLE with a Wilson-based model?*"

In [24], we partially answered this question by showing that some modifications of the Wilson AC model make it possible to predict LLE. For instance:

- We established that the Wilson model is the addition of a combinatorial Flory-type term and a residual term and that the addition of a Staverman-Guggenheim combinatorial contribution is enough to make it able to predict LLE.
- To make Wilson's model able to predict LLE, we proposed also to modify the Wilson AC model through the inclusion of an excess volume term.
- We showed that some AC models derived from Wilson's model can predict LLE. This is the case for the Orye model (built as the addition of the Wilson and Van Laar models) and the c-Wilson model, a model version proposed by Wilson himself where the AC model is simply obtained by multiplying the classical Wilson model by a constant c (≥ 1).
- More important, we showed that the TK-Wilson model, that consists essentially of the residual part of the classical Wilson model only, has the ability to predict LLE.

This last statement makes it possible to understand why the *tc*-PR-Wilson EoS, that combines the residual part of the Wilson AC model with the *tc*-PR cubic EoS, can predict liquid-liquid phase split. In [24], the case of the methanol + cyclohexane system under atmospheric pressure was used as illustration (see Fig. 1).

We however believe that more needs to be said. Indeed, it is a fact, that we will illustrate all along this article, that **the incorporation of the complete Wilson model in any CEoS by using any type of EoS/g^E mixing rule has the potential to predict LLE**. The conditions (i.e., the regions of the model parameters space) in which LLE can appear will be discussed.

Only mixing rules incorporating the full Wilson equation are considered, as only such an AC model is incapable of predicting LLE.

It is now well known that the newer formulations of the HV mixing rules that include only the residual part of the Wilson equation can predict LLE (as mentioned above and illustrated in Fig. 1 and as discussed in [24]) and therefore, they will not be considered in this article.

The aim of this article is to understand why the combination of the full Wilson model and a CEoS through EoS/g^E mixing rules allows LLE to

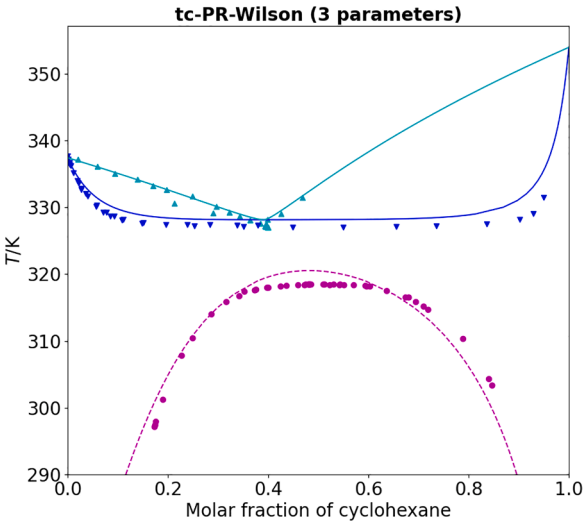

Fig. 1. Modelling of the VLE and LLE data of the system cyclohexane + methanol at atmospheric pressure from the tc-PR Wilson EoS [24].

be predicted.

2. Short presentation of the Huron-Vidal (HV) and modified Huron-Vidal (MHV) EoS/g^E mixing rules

As stated in the introduction, the approach called "EoS/g^E mixing rules" is a way to express the mixture property $\frac{a}{bRT}$ by equating the excess Gibbs energy $g^{E,\gamma}$ coming from an AC model with the corresponding property $g^{E,EoS}$ coming from an EoS at a given reference pressure (*matching equation*).

In general, these mixing rules can be written in the general form:

$$\frac{a(T,\boldsymbol{x})}{RTb(\boldsymbol{x})} = \sum_i x_i \frac{a_i(T)}{RTb_i} + \frac{E(T,\boldsymbol{x})}{C_{EoS}} \tag{2}$$

In Eq. (2), a_i and b_i are the attractive coefficient and covolume of pure-component i. $E(T,\boldsymbol{x})$ is a dimensionless excess function involving an AC model $g^{E,\gamma}(T,\boldsymbol{x})$. The relationship between E and $g^{E,\gamma}$ depends on the way used to derive the EoS/g^E mixing rule, as discussed in this section. C_{EoS} is a universal constant that depends only on the nature of the EoS and the way used to derive the mixing rule (i.e., the value of the reference pressure).

For the Huron-Vidal (HV) approach that uses an infinite reference pressure [1], the excess function is:

$$E^{HV}(T,\boldsymbol{x}) = \frac{g^{E,\gamma}(T,\boldsymbol{x})}{RT} \tag{3}$$

The two main CEoS used in practice that are the Soave-Redlich-Kwong (SRK) and Peng-Robinson (PR) EoS can be written in the following general form:

$$P = \frac{RT}{v-b} - \frac{a}{(v-r_1 b)(v-r_2 b)} \tag{4}$$

Where the r_i are two universal constants characterizing the SRK and PR EoS (see Table 1).

The universal expression for the C^{HV}_{EoS} constant as well as the particular values C^{HV}_{SRK} and C^{HV}_{PR} are:

$$C^{HV}_{EoS} = \frac{1}{r_2-r_1}\ln\left(\frac{1-r_2}{1-r_1}\right) = \begin{cases} -\ln(2) \approx -0.693 \text{ for the SRK CEoS} \\ -\frac{\sqrt{2}}{2}\ln\left(1+\sqrt{2}\right) \approx -0.623 \text{ for the PR CEoS} \end{cases} \tag{5}$$

The exact ZRP approach proposed by Michelsen does not fit into the formalism of Eq. (2). For given values of T and $\boldsymbol{x}$, the ratio $\alpha = \frac{a}{bRT}$ is obtained by solving the nonlinear Eq. (6):

$$\begin{cases} Q(\alpha) - \sum_i x_i Q(\alpha_i) = \dfrac{g^{E,\gamma}(T,\boldsymbol{x})}{RT} + \sum_i x_i \ln\left(\dfrac{b(\boldsymbol{x})}{b_i}\right) \\ \textit{with}: \; Q(z) = -1 - \ln[u(z)-1] - \dfrac{z}{r_1-r_2}\ln\left[\dfrac{u(z)-r_2}{u(z)-r_1}\right] \\ \textit{and } u(z) = \dfrac{2(r_1 r_2 + z)}{r_1+r_2+z+\sqrt{(r_1+r_2+z)^2 - 4(r_1 r_2+z)}} \end{cases} \tag{6}$$

With: $\alpha_i = \frac{a_i}{b_i RT}$. Note that the expression of $u(z)$ in Eq. (6) is only defined for:

$$z \geq -r_1 - r_2 + 2 + 2\sqrt{1 - r_1 - r_2 + r_1 r_2}, \text{ with } z \in \{\alpha, \alpha_i\} \tag{7}$$

In practice, the consequence of this limitation is the impossibility to apply the exact ZRP mixing rule at high temperature.

The MHV1 approach, also introduced by Michelsen, uses a linear approximation of the Q function with respect to α, which removes the temperature limitation from the application range of the exact ZRP approach. MHV1 fits into the formalism of Eq. (2). In such a case, the excess function is written:

$$E^{MHV1}(T,\boldsymbol{x}) = \frac{g^{E,\gamma}(T,\boldsymbol{x})}{RT} + \sum_i x_i \ln\left(\frac{b}{b_i}\right) \tag{8}$$

And the corresponding universal constants are:

$$C^{MHV1}_{EoS} = \begin{cases} -0.593 \text{ for the SRK CEoS} \\ -0.530 \text{ for the PR CEoS} \end{cases} \tag{9}$$

The MHV2 approach consists in approximating the Q function as a quadratic function of $\alpha = \frac{a}{bRT}$. For the present study, using the exact ZRP or the MHV2 approach would not alter the general conclusions we will draw from the MHV1 approach. For this reason, we will consider only the MHV1 approach in the remainder of this article.

In addition to the mixing rules for the parameter $a/(RTb)$, a mixing rule for the covolume $b(\boldsymbol{x})$ must be chosen. While the ZRP approach allows a free choice of the mixing rule for b, the Huron and Vidal requires the use of a linear mixing rule for b [1].

3. Detection of LLE in binary systems

3.1. On the instability of liquid phases

The instability criterion is used to detect the presence of LLE in binary systems at given temperature T and pressure P. It can be stated as follows [31]:

*A liquid binary mixture is said to be "unstable at given temperature T and pressure P" (*i.e.*, it exhibits a liquid-liquid separation domain at (T,P)) if there exists a range of the molar fraction x_1 such that the property Γ_g (defined in Eq. (10))* is negative.

$$\Gamma_g := \left(\frac{\partial^2\left(\frac{g^M}{RT}\right)}{\partial x_1^2}\right)_{T,P} \tag{10}$$

*Conversely, if for any molar fraction $x_1 \in [0;1]$, Γ_g is positive, a liquid binary mixture is said to be "stable at given temperature T and pressure P" (*i.e.*, it does not exhibit a liquid-liquid phase separation at (T,P), whatever being the composition).*

The composition domain where the fluid exhibits instability is associated with negative values of Γ_g (see the dotted lines in Fig. 2b), and therefore, corresponds to concave parts of the curve $\frac{g^M}{RT}$ versus molar fraction x_1 at (T,P) (see the dotted lines in Fig. 2a).

Alternatively, the criterion for detecting liquid instability at (T,P) mentioned above can be written in a more concise form involving the sign of the minimum Ψ of the function Γ_g (see the black triangle in Fig. 2b):

- If $\Psi(T,P) < 0$, the fluid is unstable at (T,P), i.e., there exists a liquid-liquid phase split,
- Otherwise, if $\Psi(T,P) \geq 0$, it is stable at (T,P).

Where Ψ is defined as:

$$\Psi(T,P) = \min_{x_1 \in [0;1]} \Gamma_g \tag{11}$$

This mathematical form of the instability criterion is used in the following.

Table 1
Universal constants r_i of the PR and SRK CEoS.

	SRK	PR
r_1	-1	$-1-\sqrt{2}$
r_2	0	$-1+\sqrt{2}$

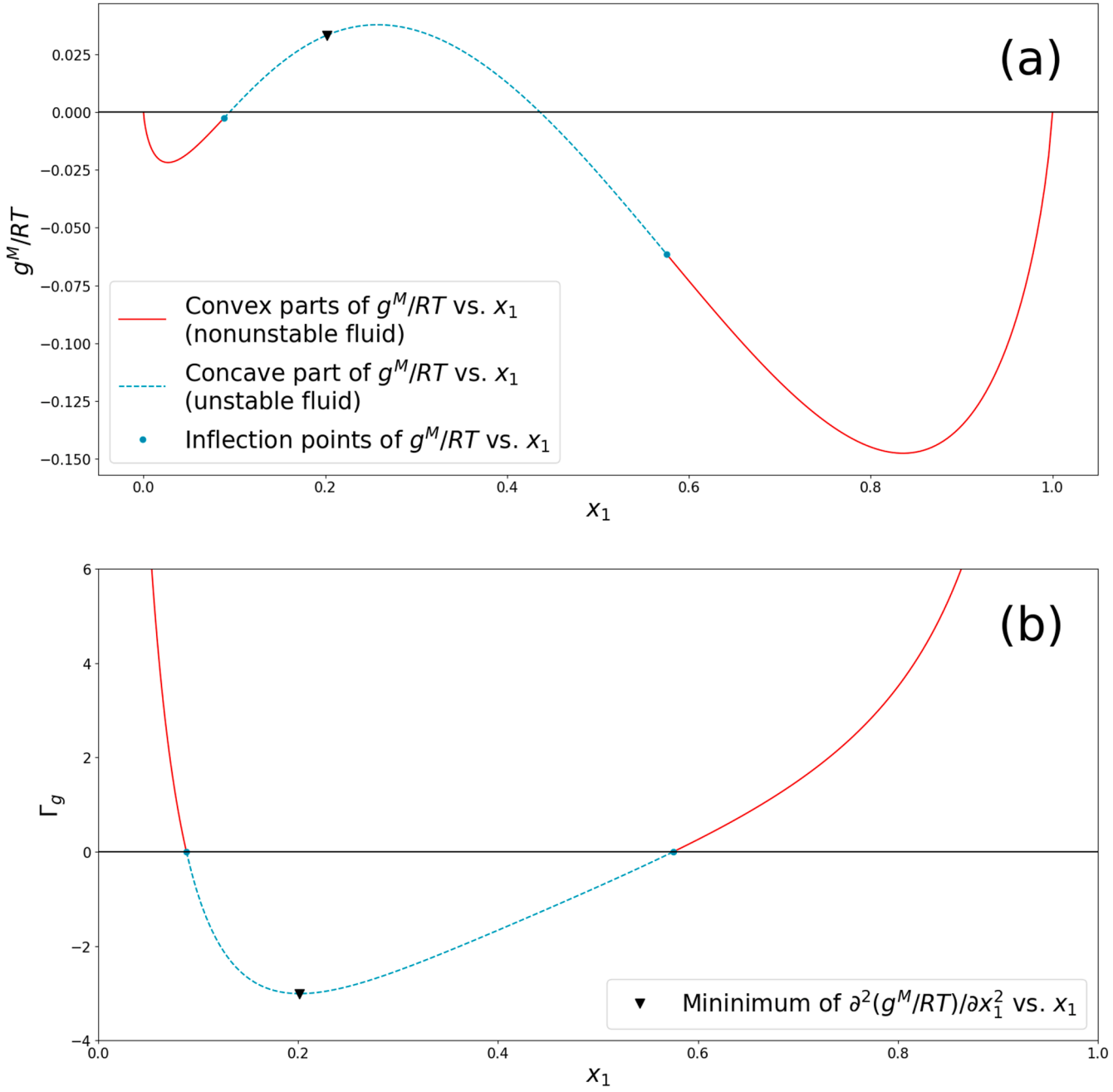

Fig. 2. Graphical illustration of the instability criterion in binary systems at a specified temperature and pressure: (a) in the plane $g^M/(RT)$ vs. molar fraction x_1 and (b) in the plane Γ_g vs. molar fraction x_1 (where Γ_g, defined in Eq. (10), denotes the 2nd derivative of $g^M/(RT)$ with respect to x_1). The unstable region is associated with the concave part (dotted line) of the curve $\frac{g^M}{RT}$ vs. molar fraction x_1. The non-unstable region aggregates stable and metastable states and is associated with convex parts (continuous lines) of the curve $\frac{g^M}{RT}$ vs. molar fraction x_1. The $\frac{g^M}{RT}$ curve was plotted with an arbitrary AC model (Van Laar) and the binary interaction parameters $A_{12} = 2\ J/mol$ and $A_{21} = 4\ J/mol$.

3.2. *Calculation of the Gibbs energy change on mixing from a CEoS*

To calculate the Gibbs energy change on mixing $g^{M,EoS}$, the relation between $g^{M,EoS}$ and $g^{E,EoS}$, Eq. (12), can be used.

$$\frac{g^M}{RT} = \frac{g^{M,id}}{RT} + \frac{g^E}{RT} \tag{12}$$

Where $g^{M,id}$ is the ideal solution Gibbs energy change on mixing.

In the case (valid all along this paper) where the mixture phase and the pure components are all liquid at the T and P considered, $g^{M,id}$ is obtained from:

$$\frac{g^{M,id}}{RT} = x_1 \ln x_1 + x_2 \ln x_2 \tag{13}$$

In practice, the plotting of the curves $\frac{g^M}{RT}$ versus x_1 at (T,P), that are shown abundantly in the next sections, obeys the following calculation procedure:

- Specify (T,P).
- Calculate v_i by solving the CEoS (4) applied to pure component i at (T, P). If the CEoS has 3 roots, select the liquid-like root.

- Vary x_1 between 0 and 1 in steps of Δx (e.g., $\Delta x = 0.001$). For each value of x_1:
  - Calculate v by solving the CEoS (4) for mixture at (T, P, x_1). As previous, if the CEoS has 3 roots, select the stable one, i.e., the one showing the lowest fugacity.
  - Calculate $\frac{g^{M,EoS}}{RT}$ using Eq. (12) and the expressions introduced in the next section (Eq. (21) in particular).

4. An attempt to answer the question posed in the title by mathematical analysis of the expression $g^{E,EoS}$

4.1. The Wilson AC model

The Wilson model plays an essential role here. When, in the title of this article, we ask the question "Can liquid-liquid equilibria be predicted by the combination of a cubic equation of state and a g^E model not suitable for liquid-liquid equilibria?", we are clearly aiming at the Wilson AC model, which is notorious for not being able to predict LLE [24].

The expression of the complete Wilson AC model for a binary system is given by Eq. (14). Generally, the molar volumes v_i and v_j of pure components i and j present in the $\Lambda_{ji}(T)$ function are taken at 298.15 K.

$$\begin{cases} \dfrac{g^{E,\gamma}}{RT} = -x_1\ln[x_1 + x_2\Lambda_{21}(T)] - x_2\ln[x_2 + x_1\Lambda_{12}(T)] \\ \Lambda_{ji}(T) = \dfrac{v_j}{v_i}\exp\left(-\dfrac{A_{ji}}{T}\right) \\ A_{ij} = \lambda_{ij} - \lambda_{jj} \text{ with } \lambda_{ij} = \lambda_{ji} \\ \Lambda_{ii} = \Lambda_{jj} = 1 \end{cases} \tag{14}$$

In a previous study [24], we showed how the residual and combinatorial parts of the AC model can be derived from its overall expression and arrived at Eq. (15).

$$\begin{cases} \dfrac{g^{E,\gamma}}{RT} = \dfrac{g^{E,\gamma}_{comb}}{RT} + \dfrac{g^{E,\gamma}_{res}}{RT} \\ \dfrac{g^{E,\gamma}_{comb}}{RT} = x_1\ln\left(\dfrac{\Phi_1}{x_1}\right) + x_2\ln\left(\dfrac{\Phi_2}{x_2}\right) \\ \dfrac{g^{E,\gamma}_{res}}{RT} = -x_1\ln\left[\Phi_1 + \Phi_2\exp\left(-\dfrac{A_{21}}{T}\right)\right] - x_2\ln\left[\Phi_2 + \Phi_1\exp\left(-\dfrac{A_{12}}{T}\right)\right] \\ \text{with : } \Phi_i = \dfrac{x_i v_i}{\sum_j x_j v_j} \end{cases} \tag{15}$$

In the Appendix C of the same study [24], we showed that any AC model which can be written in the general form:

$$\frac{g^{E,\gamma}}{RT} = -x_1\ln(a_1x_1 + b_1) - x_2\ln(a_2x_1 + b_2) \tag{16}$$

cannot predict LLE. Here, a_i and b_i are constant model parameters.

The demonstration consisted simply in expressing the Gibbs energy change on mixing $g^M/(RT)$ (using Eq. (12)) and differentiating it twice in succession with respect to x_1 in order to obtain Γ_g.

$$\Gamma_g = \frac{b_1^2}{x_1(a_1x_1 + b_1)^2} + \frac{(a_2 + b_2)^2}{x_1(a_2x_1 + b_2)^2} \tag{17}$$

It can be seen that Γ_g is necessarily found positive for any $x_1 \in [0;1]$. The Wilson model fits into the formalism of Eq. (16). Indeed, by setting:

$$\begin{cases} a_1 = 1 - \Lambda_{21} \\ b_1 = \Lambda_{21} \\ a_2 = \Lambda_{12} - 1 \\ b_2 = 1 \end{cases} \tag{18}$$

the Wilson AC model is obtained.

This is the simple reason why the Wilson model will never predict LLE: its mathematical form excludes the possibility for the second derivative of $\frac{g^M}{RT}$ to become negative.

The combinatorial (Flory type) part of Wilson (see Eq. 15) fits also into the formalism of Eq. (16), and consequently, an athermal solution modelled with the Wilson expression cannot predict LLE either.

The residual part of Wilson (see Eq. 15) is known as the "TK-Wilson" model. This specific model contribution is known however to have the ability to predict LLE [24].

Does the mathematical form of $g^{E,EoS}$ – obtained by combining a CEoS and the complete Wilson model through the HV or ZRP mixing rules – fits into the formalism of Eq. (16) and therefore, could not predict LLE? Let us answer this question by analyzing the $g^{E,EoS}$ expression.

4.2. Analysis of $g^{E,EoS}$

For a CEoS defined by Eq. (4), the molar excess Gibbs energy $g^{E,EoS}$ is expressed by Eq. (19) [32].

$$\begin{aligned} \frac{g^{E,EoS}(T,P,\boldsymbol{x})}{RT} &= \frac{a^E(T,P,\boldsymbol{x})}{RT} + \frac{P\cdot v^E(T,P,\boldsymbol{x})}{RT} \\ &= \frac{a^{TP-\text{res}}(T,P,\boldsymbol{x})}{RT} - \sum_i x_i\frac{a_i^{TP-\text{res}}(T,P)}{RT} + \frac{P\cdot v^E(T,P,\boldsymbol{x})}{RT} \end{aligned} \tag{19}$$

With: $\frac{a^{TP-\text{res}}}{RT} = -RT\ln\left[\frac{P(T,v,\boldsymbol{x})\cdot v}{RT}\right] - \int_{+\infty}^{v}\left(\frac{P(T,v,\boldsymbol{x})}{RT} - \frac{1}{v}\right)dv$. To avoid confusion between the different types of "residual" properties, let us clarify our notations. The "*TP-res*" label is used to denote a *departure* property, i.e., the difference between a real-mixture property at $(T,P,\boldsymbol{x})$ and the corresponding property of a perfect gas at $(T,P,\boldsymbol{x})$. A residual property labelled with "*res*" here denotes the *enthalpic* contribution of a CEoS or an AC model. It is the opposite of a *combinatorial* ("*comb*") property reflecting the *entropic* contribution.

If the CEoS (Eq. (4)) is divided into repulsive and attractive parts as done in Eq. (20), the combinatorial and residual contributions to $g^{E,EoS}$ can be identified: the combinatorial part is the quantity $a^E/(RT)$ derived from the repulsive EoS term while the residual term is the one derived from the attractive part of the CEoS.

$$\begin{cases} P = P_{comb} + P_{res} \\ \text{Repulsive EoS term : } P_{comb} = \dfrac{RT}{v-b} \\ \text{Attractive EoS term : } P_{res} = -\dfrac{a}{(v-r_1b)(v-r_2b)} \end{cases} \tag{20}$$

By combining Eqs. (19) and (20), the general expression (21), valid for any CEoS, is obtained.

$$\begin{cases} \dfrac{g^{E,EoS}}{RT} = \dfrac{a^{E,EoS}_{comb}}{RT} + \dfrac{a^{E,EoS}_{res}}{RT} + \dfrac{Pv^{E,EoS}}{RT} \\ \dfrac{a^{E,EoS}_{comb}}{RT} = \displaystyle\sum_{i=1}^{2} x_i\ln\left(\frac{v_i - b_i}{v-b}\right) \\ \dfrac{a^{E,EoS}_{res}}{RT} = \displaystyle\sum_{i=1}^{2} x_i\frac{a_i}{b_iRT(r_1-r_2)}\ln\left(\frac{v_i - r_2b_i}{v_i - r_1b_i}\right) - \frac{a}{bRT(r_1-r_2)}\ln\left(\frac{v-r_2b}{v-r_1b}\right) \\ v^E = v - \displaystyle\sum_i x_iv_i \end{cases} \tag{21}$$

If the HV or MHV1 mixing rule are used to express $a/(bRT)$, Eq. (22) is obtained:

$$\begin{cases} \dfrac{g^{E,EoS}}{RT} = \dfrac{a^{E,EoS}_{comb}}{RT} + \dfrac{a^{E,EoS}_{res}}{RT} + \dfrac{Pv^{E,EoS}}{RT} \\ \dfrac{a^{E,EoS}_{comb}}{RT} = \sum_{i=1}^{2} x_i \ln\left(\dfrac{v_i - b_i}{v - b}\right) \\ \dfrac{a^{E,EoS}_{res}}{RT} = \dfrac{1}{r_1 - r_2} \sum_{i=1}^{2} x_i \dfrac{a_i}{b_i} \left[\ln\left(\dfrac{v_i - r_2 b_i}{v_i - r_1 b_i}\right) - \ln\left(\dfrac{v - r_2 b}{v - r_1 b}\right) \right] \\ \quad - \dfrac{\dfrac{g^{E,\gamma}}{RT} + k \sum_{i=1}^{2} x_i \ln\left(\dfrac{b}{b_i}\right)}{(r_1 - r_2) C^{HV \text{ or } MHV1}_{EoS}} \ln\left(\dfrac{v - r_2 b}{v - r_1 b}\right) \\ \text{with : } k = \begin{cases} 0 \text{ for HV} \\ 1 \text{ for MHV1} \end{cases} \end{cases} \tag{22}$$

By comparing Eqs. (22) and (16), it becomes obvious that the mathematical expressions of the g^E from the AC model and from the CEoS are completely different. In particular, it can be observed that:

- $\frac{a^{E,EoS}_{comb}}{RT}$ (Eq. (22)) is significantly different from $\frac{g^{E,\gamma}_{comb}}{RT}$ (Eq. (15)). The first is a free-volume term (i.e., a modified Flory term where volumes v are replaced by free volumes, $v - b$) while the second is a classical Flory term expressed in terms of molar volumes (v), but, more important, the composition dependency of the EoS combinatorial term is much more complex than the composition dependency of the AC combinatorial term. In the AC model, the molar volume of the mixture is approximated as a linear function of the composition ($v = \sum_i x_i v_i(298.15\text{ K})$) thus neglecting the excess volume contribution as well as temperature effects. In the EoS, the molar volume is obtained by solving the CEoS at $(T, P, \boldsymbol{x})$ with a composition dependency hidden in the expressions of the parameters a and b of the CEoS.
- The mathematical form of the residual term of the AC model, $\frac{g^{E,\gamma}_{res}}{RT}$ (Eq. (15)), consists of logarithmic terms weighted by molar fractions. The mathematical expression of the combinatorial term produced by the CEoS, $\frac{a^{E,EoS}_{res}}{RT}$ (Eq. (22)), cannot be written in a similar form.
- The $\frac{Pv^{E,EoS}}{RT}$ term of the CEoS has no equivalent in the AC model (which assumes $v^{E,\gamma} = 0$).

In conclusion, a basic analysis of the expressions of the g^E functions shows that:

- Wilson's model cannot predict LLE because of its mathematical form. This impossibility cannot be explained by fundamental physico-chemical causes.
- The expression of $g^{E,EoS}$ obtained by combining the Wilson model and a CEoS is very different from Wilson's model expression. In other words, the expression of $\frac{g^{E,EoS}}{RT}$ cannot be recast into the form of Eq. (16).

If $\frac{g^{E,EoS}}{RT}$ and Wilson's model had the same mathematical form (Eq. (16)), it could be possible to immediately conclude that the EoS cannot predict LLE. Since we observe that this is not the case, nothing can be concluded regarding the capacity of the EoS to predict LLE.

However, it could be claimed that when using the EoS/g^E approach, the matching equation constraints the $g^{E,EoS}$ to be identical to $g^{E,Wilson}$ at the temperature, pressure and composition of the matching conditions. Therefore, at the matching pressure ($+\infty$ for the Huron-Vidal approach and ≈ 0 for MHV1 which is an approximate ZRP approach), $g^{E,EoS} = g^{E,Wilson}$ and the EoS cannot predict LLE as Wilson's model cannot. Nevertheless, there is no evidence that this statement holds in other conditions of pressure.

In the next section, it is shown using two binary systems as examples, that the CEoS/Wilson model can produce LLE. We consider that this illustration has evidential value.

5. Proof by examples

In this section, the HV and MHV1 mixing rules combined with the complete Wilson model are considered. All the calculations were performed with the PR CEoS applied to a given binary system, the properties of which were chosen in order to make the phenomena well visible and illustrative. However, note that the results shown here are fully general and do not depend on the EoS selection. The components of the binary systems used in our calculations have the properties reported in Table 2.

5.1. First observations with the ethane(1) + toluene(2) system

In this section, two models are considered: the PR-HV-Wilson EoS (EoS combining HV mixing rule incorporating the complete Wilson model) and the PR-MHV1-Wilson EoS (the MHV1 mixing rule is used in this case). In both cases, a linear mixing rule is used for the covolume.

The values of the binary interaction parameters (Bips) A_{12} and A_{21} were searched in order to generate a liquid-phase splitting at $T = 280$ K and $P = 3.00$ MPa. These (T, P) conditions were arbitrarily selected for the calculations. A grid-based parameter search in the (A_{12}, A_{21}) space was implemented and the Ψ function, defined in Eq. (11), was estimated in each point of the grid. Fig. 3 shows the regions of positive and negative Ψ associated with the absence and the presence of LLE, respectively.

Fig. 3 thus provides evidence that the incorporation of the complete Wilson AC model which cannot predict liquid instability within a CEoS does not prevent the CEoS from predicting LLE. To deepen the analysis and understand which terms of the EoS are responsible for the presence of LLE, let us now consider a specific set of (A_{12}, A_{21}) parameters that produces LLE. The Bips values in Eq. (23) (corresponding to the star symbol in the parameter space shown in the left panel of Fig. 3) were selected to compare and analyse the similarities and differences between $(g^{E,EoS}, g^{M,EoS})$ and $(g^{E,\gamma}, g^{M,\gamma})$ as well as between their respective combinatorial and residual contributions:

$$A_{12} = A_{21} = 1000\text{ K} \tag{23}$$

The Gibbs energy change on mixing and excess Gibbs energy plots (including the plots of the combinatorial and residual contributions), calculated from the Wilson AC model at $T = 280$ K, are shown in Fig. 4.

As expected, it can be observed that the Gibbs energy on mixing curve predicted by the Wilson model is convex over the entire composition range, indicating that the liquid phase remains stable. The proximity of the molar volumes of the two pure compounds at 298.15 K ($v_2/v_1 \approx 1.12$) makes the combinatorial contribution very small and, as a consequence, the excess Gibbs energy of the system contains essentially a residual contribution.

Fig. 5 enables to compare the g^E and g^M functions obtained from the AC model and the CEoS PR-HV-Wilson. First, it can be seen that the $g^{E,\gamma}$ (AC model) and $g^{E,EoS}$ functions are similar, both qualitatively and in magnitude, which is not surprising since the HV mixing rule dictates their strict equality at infinite pressure. In the present case, the pressure is 3 MPa and is therefore not infinite, but the constraint at infinite pressure tends to bring the curves close together under high pressure conditions. However, in contrast to the g^E functions, it can be seen that the $g^{M,EoS}$ and $g^{M,\gamma}$ curves are significantly different: the $g^{M,\gamma}$ curve is convex over the whole composition range while the $g^{M,EoS}$ curve exhibits a wave shape with a concave part revealing the instability of the liquid phase. In such a case, the double-tangent construction of coexisting phases [34] can be used to determine the compositions of the two liquid phases in equilibrium. The key question we now need to address is: *why is there such a difference between the $g^{M,EoS}$ and $g^{M,\gamma}$ curves?*

Note that the g^E functions ($g^{E,EoS}$ and $g^{E,\gamma}$) are both positive and

Table 2
Physical properties of the pure components of the binary systems considered in Section 0.

	Ethane	Toluene	Methanol	Cyclohexane
T_c/K (critical temperature)	305.32	591.75	512.5	553.8
P_c/MPa (critical pressure)	4.872	4.108	8.084	4.080
ω (acentric factor)	0.0995	0.264	0.566	0.2081
$v(298.15\ \mathrm{K})/\left(\mathrm{m^3{\cdot}mol^{-1}}\right)$ (saturated-liquid molar volume, source: DIPPR [33])	$9.536{\cdot}10^{-5}$	$1.067{\cdot}10^{-4}$	$4.058{\cdot}10^{-5}$	$1.0886{\cdot}10^{-4}$

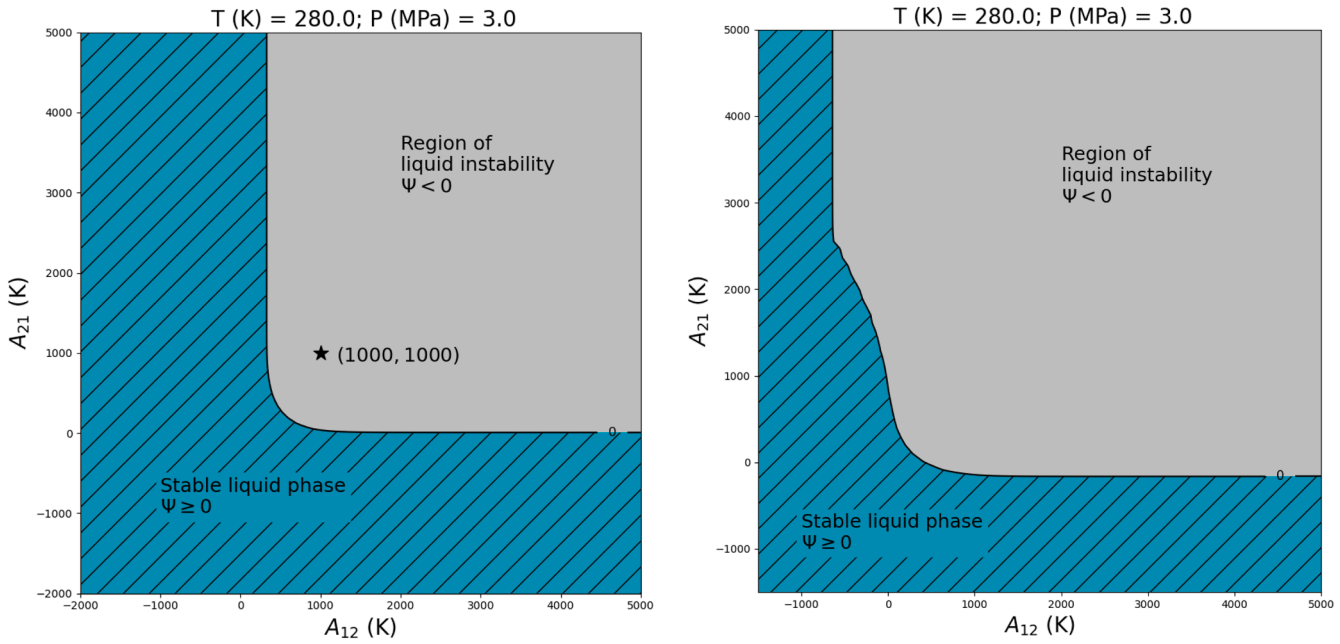

Fig. 3. Sign of the Ψ function, defined by Eq. (11) in the parameter space $(\boldsymbol{A}_{12}, \boldsymbol{A}_{21})$ for the system ethane(1) + toluene(2) at 280 K and 3 MPa modelled with the PR-HV-Wilson model (left side) and the PR-MHV1-Wilson model (right side). Hatched area: regions of stable liquid phases ($\boldsymbol{\Psi} \geq 0$). Non-hatched area: unstable liquid phases ($\boldsymbol{\Psi} < 0$). (★) Point characterizing the parameter set selected to illustrate the ability of the model to predict LLE in Section 4.3.

opposite in sign to the ideal Gibbs energy change on mixing ($g^{M,id} = RT\sum_i x_i \ln x_i$). In addition, the functions $g^{E,EoS}$, $g^{E,\gamma}$ and $-g^{M,id}$ are of the same order of magnitude in absolute value and produce curves that are very similar in shape. On the contrary, the g^M functions ($g^{M,EoS}$ and $g^{M,\gamma}$), which result both from the addition of a positive g^E term and a negative $g^{M,id}$ term, have very different shapes and are one order of magnitude smaller than g^E functions. This shows that small differences between $g^{E,EoS}$ and $g^{E,\gamma}$ can generate important deviations between $g^{M,EoS}$ and $g^{M,\gamma}$. For a more detailed analysis of this system modelled with the PR-HV-Wilson EoS and Wilson's AC model, including the comparison between their residual and combinatorial contributions, the reader is reffered to Appendix 1.

Before closing the discussion on the ethane + toluene system, it seems interesting to ask whether the PR-Wilson type models (PR-HV-Wilson and PR-MHV1-Wilson) show a general or specific behaviour. In other words, would we obtain a map similar to that shown in Fig. 3 if the Wilson model were replaced by, for example, the NRTL model [35]? Our calculations show that the PR-Wilson models are quite similar to other models formed in a similar way (i.e. by incorporating an activity coefficient model into the PR EoS through HV or MHV1 mixing rules). To illustrate this statement, the maps shown in Fig. 3 have been recalculated using the PR-HV-NRTL and PR-MHV1-NRTL models. The results are presented in Appendix 2.

5.2. Second observations with the methanol(1) + cyclohexane(2) system

The first observations of Section 4.3 could invite us to think that LLE can always be predicted from a CEoS embedding the Wilson AC model at the condition that specific and high enough values of the binary interaction parameters A_{ij} are used. This is actually not so simple and to illustrate this statement, the case of the methanol + cyclohexane system is now addressed. As previous, the two modelling strategies PR-HV-Wilson and PR-MHV1-Wilson were considered. The results are presented in Fig. 6.

When the PR-MHV1-Wilson EoS is used, the same observations as previous can be made: LLE is produced for high values of the binary parameters A_{12} and A_{21}. However, when the PR-HV-Wilson EoS is used, it is no longer possible to get LLE, regardless of the values assigned to (A_{12}, A_{21}).

To better understand in which conditions LLE can be observed, a deeper analysis of the general expressions of the Gibbs energy change on mixing coming from the PR-Wilson EoS is required.

6. Analytical study of the $g^{M,EoS}$ property

As mentioned above, the Gibbs energy change on mixing $g^{M,EoS}$ results from 4 different contributions: a combinatorial term a^E_{comb}, a residual term a^E_{res}, a Pv^E term (see Eqs. (12) and (22)) and a term expressing the Gibbs energy on mixing of an ideal solution denoted $g^{M,id}$ (see Eq. (12)). The capacity of an EoS to predict LLE is narrowly linked to the sign of the second derivative of $g^{M,EoS}/(RT)$ as highlighted in Section 3.1. After some algebra, one obtains:

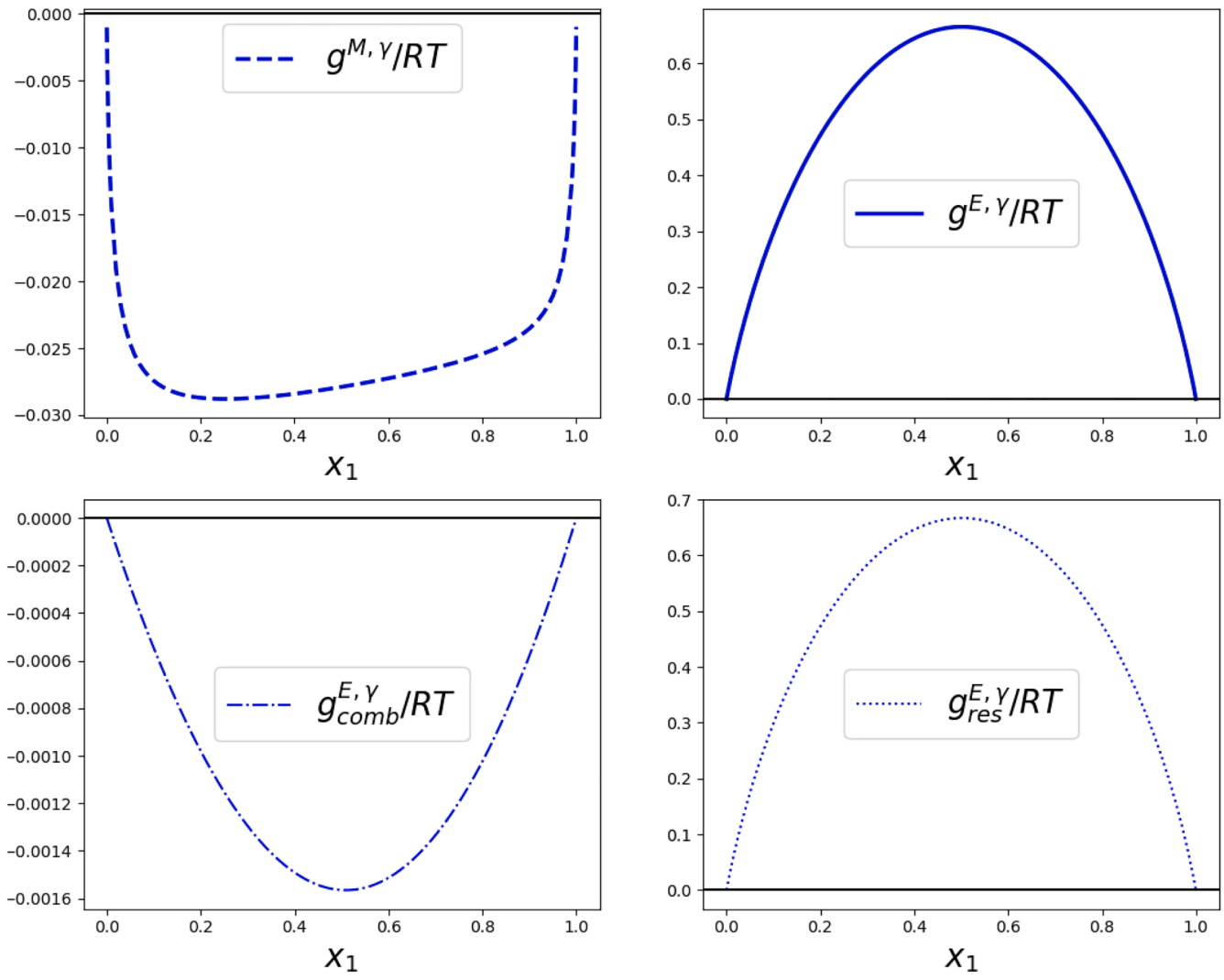

Fig. 4. Representation of $\boldsymbol{g^{M,\gamma}/RT}$, $\boldsymbol{g^{E,\gamma}/RT}$, $\boldsymbol{g^{E,\gamma}_{comb}/RT}$ and $\boldsymbol{g^{E,\gamma}_{res}/RT}$ for the system ethane(1) + toluene(2) at 280 K modelled with the complete Wilson AC model and parameters (23).

$$
\begin{cases}
\left(\dfrac{\partial^2 \frac{g^{M,EoS}}{RT}}{\partial x_1^2}\right)_{T,P} = \dfrac{1}{x_1 x_2} + \left(\dfrac{\partial^2 \frac{a^{E,EoS}_{comb.}}{RT}}{\partial x_1^2}\right)_{T,P} + \left(\dfrac{\partial^2 \frac{a^{E,EoS}_{res.}}{RT}}{\partial x_1^2}\right)_{T,P} + \dfrac{Pv_{xx}}{RT} \\
\left(\dfrac{\partial^2 \frac{a^{E,EoS}_{comb.}}{RT}}{\partial x_1^2}\right)_{T,P} = \left(\dfrac{v_x - b_x}{v-b}\right)^2 - \dfrac{v_{xx} - b_{xx}}{v-b} \\
\left(\dfrac{\partial^2 \frac{a^{E,EoS}_{res.}}{RT}}{\partial x_1^2}\right)_{T,P} = \left(x_1 \dfrac{a_1}{RTb_1} + x_2 \dfrac{a_2}{RTb_2} + \dfrac{E}{C_{EoS}}\right) \\
\left[\dfrac{(bv_{xx} - vb_{xx})}{(v-r_1 b)(v-r_2 b)} + \dfrac{[(-2r_1 r_2 b + v(r_1+r_2))b_x + ((r_1+r_2)b - 2v)v_x](bv_x - vb_x)}{(v-r_1 b)^2 (v-r_2 b)^2}\right] \\
+ \dfrac{2(bv_x - vb_x)\left(\dfrac{a_1}{RTb_1} - \dfrac{a_2}{RTb_2} + \dfrac{E_x}{C_{EoS}}\right)}{(v-r_1 b)(v-r_2 b)} - \dfrac{E_{xx}}{(r_1 - r_2)C_{EoS}} \ln\left(\dfrac{v-r_2 b}{v-r_1 b}\right)
\end{cases}
\tag{24}
$$

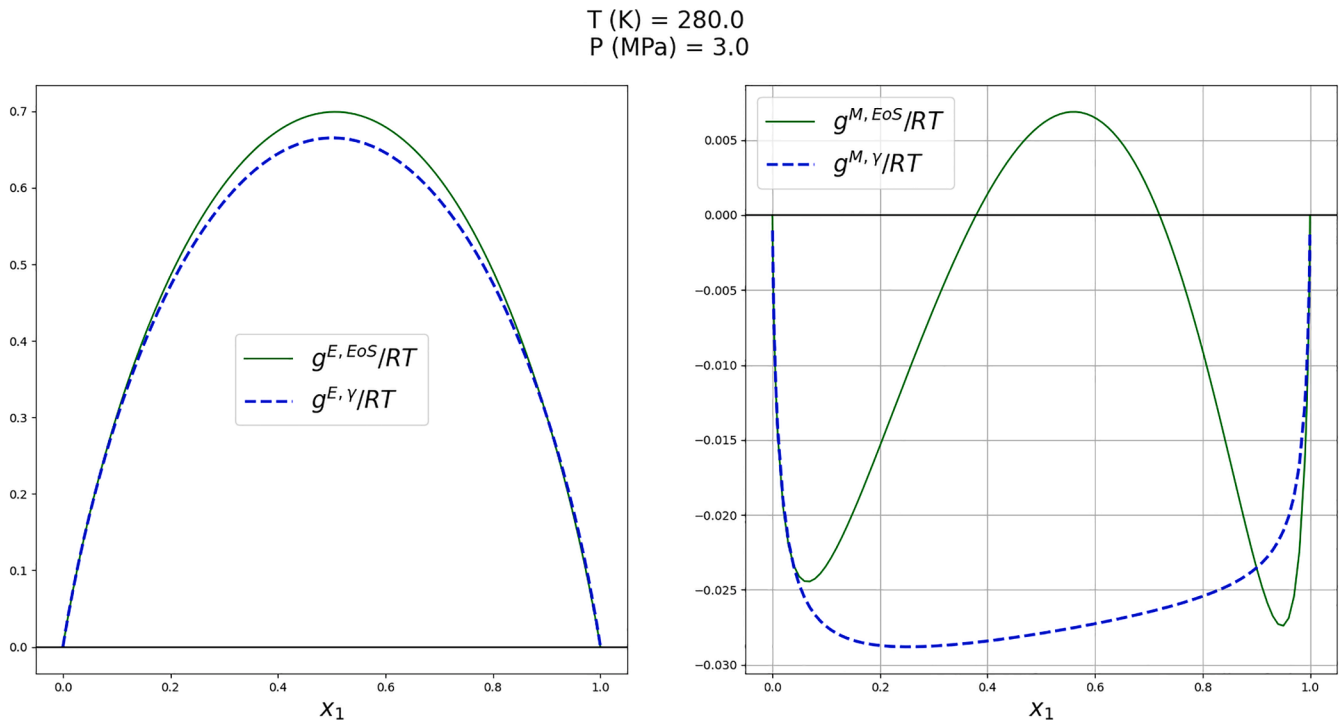

Fig. 5. System ethane(1) + toluene(2) at 280 K and 3 MPa. Representation of the $\boldsymbol{g^M/RT}$ and $\boldsymbol{g^E/RT}$ curves modelled with the complete Wilson AC model (γ) and the PR-HV-Wilson EoS.

Where subscript x and xx denote the first and second derivatives of the property at fixed temperature and pressure. The E, E_x and E_{xx} quantities are defined in Eq. (25).

$$\begin{cases} E = \dfrac{g^{E,\gamma}}{RT} + k\sum_{i=1}^{2} x_i \ln\left(\dfrac{b}{b_i}\right) \text{ with : } k = \begin{cases} 0 \text{ for HV} \\ 1 \text{ for MHV1} \end{cases} \\ E_x = \left(\dfrac{\partial E}{\partial x_1}\right)_{T,P} = \left(\dfrac{\partial \frac{g^{E,\gamma}}{RT}}{\partial x_1}\right)_{T} + k\left[\ln\left(\dfrac{b_2}{b_1}\right) + \dfrac{b_x}{b}\right] \\ E_{xx} = \left(\dfrac{\partial^2 E}{\partial x_1^2}\right)_{T,P} = \left(\dfrac{\partial^2 \frac{g^{E,\gamma}}{RT}}{\partial x_1^2}\right)_{T} + k\left[\dfrac{b_{xx}}{b} - \left(\dfrac{b_x}{b}\right)^2\right] \end{cases} \tag{25}$$

It is recalled that the attractive parameter a_i of the pure component i appearing in Eq. (24) is the product of the critical parameter $a_{c\,i}$ and a temperature dependent function (the Soave alpha function) which involves the acentric factor ω_i and the critical temperature of i. The property $\left(\frac{\partial^2 \frac{g^{M,EoS}}{RT}}{\partial x_1^2}\right)_{T,P}$ can be seen as a function of a list of 13 parameters as highlighted by Eq. (26)).

$$\left(\frac{\partial^2 \frac{g^{M,EoS}}{RT}}{\partial x_1^2}\right)_{T,P} = f\left(T, P, \boldsymbol{x}, b_1, b_2, a_{c1}, a_{c2}, v_1, v_2, \frac{A_{12}}{T}, \frac{A_{21}}{T}, \omega_1, \omega_2\right) \tag{26}$$

Where v_1 and v_2 are the molar volumes of the pure compounds at 298.15 K; the A_{ij}/T are the binary interaction parameters, all of which are involved in the expression of Wilson's model (see Eq. (14)). Following the corresponding state principle, it is possible to reduce the number of parameters involved in Eq. (26) by replacing dimensional parameters by dimensionless properties. Reduced temperature and pressure are defined by dividing the temperature and pressure by the critical properties of component 1 of the binary system (generally defined as the component with the lowest critical temperature):

$$T_r = T/T_{c1} \text{ and } P_r = P/P_{c1} \tag{27}$$

Eq. (26) becomes:

$$\left(\frac{\partial^2 \frac{g^{M,EoS}}{RT_{c1}}}{\partial x_1^2}\right)_{T,P} = f\left(T_r, P_r, \boldsymbol{x}, \frac{b_2}{b_1}, \frac{a_{c2}}{a_{c1}}, \frac{v_2}{v_1}, \frac{A_{12}}{T}, \frac{A_{21}}{T}, \omega_1, \omega_2\right) \tag{28}$$

The reduced property $\left(\frac{\partial^2 \frac{g^{M,EoS}}{RT_{c1}}}{\partial x_1^2}\right)_{T,P}$ now depends on 10 parameters. At given reduced temperature and pressure, the minimum of the quantity $\left(\frac{\partial^2 \frac{g^{M,EoS}}{RT_{c1}}}{\partial x_1^2}\right)_{T,P}$ with respect to the composition is now denoted Ψ_r (index r stands for reduced / dimensionless property), as defined in Eq. (29).

$$\begin{cases} (T_r, P_r) \text{ specified} \\ \Psi_r\left(\dfrac{b_2}{b_1}, \dfrac{a_{c2}}{a_{c1}}, \dfrac{v_2}{v_1}, \dfrac{A_{12}}{T}, \dfrac{A_{21}}{T}, \omega_1, \omega_2\right) = \min_{x}\left(\dfrac{\partial^2 \frac{g^{M,EoS}}{RT_{c1}}}{\partial x_1^2}\right)_{T,P} \end{cases} \tag{29}$$

When $\Psi_r = 0$, the liquid phase of the binary system is near to become unstable. Consequently, the curve $g^{M,EoS}/(RT_{c1})$ versus x_1 plotted at given (T_r, P_r) and for a given mixture is convex over the complete composition range but shows a single inflection point. Regardless of the type of representation used (i.e., regardless which parameter is plotted against which parameter), the locus of points satisfying $\Psi_r = 0$ is always a boundary between regions where Ψ_r is positive (corresponding to stable liquid phases) and regions where Ψ_r is negative (corresponding to unstable liquid phases, i.e., LLE). Such types of curves have been plotted

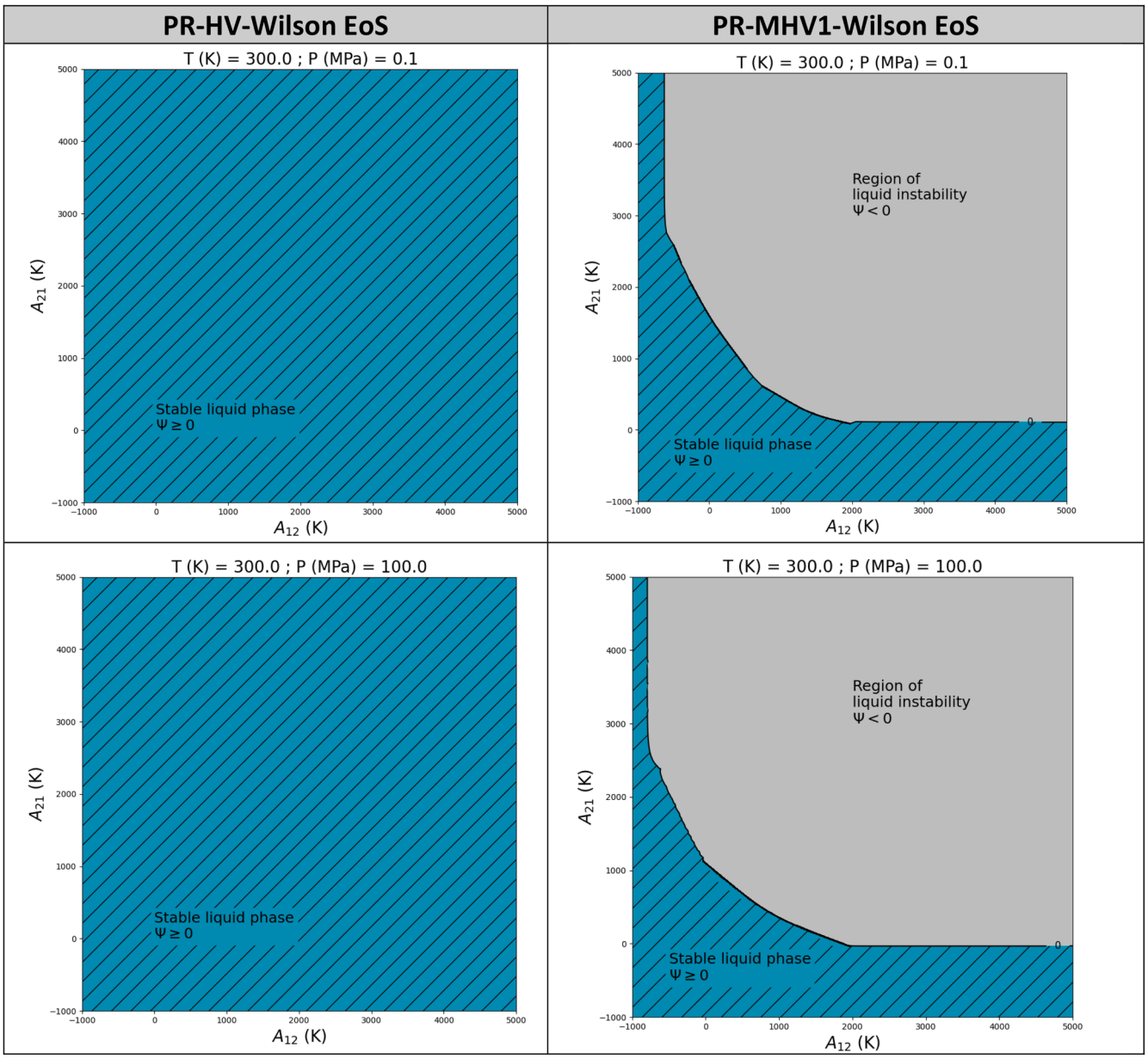

Fig. 6. Regions of liquid stability and liquid instability for the system methanol(1) + cyclohexane(2) at 300 K and pressure set to 0.1 MPa (above) and 100 MPa (below), modelled with the PR-HV-Wilson EoS (left side) and the PR-MHV1-Wilson model (right side). Hatched area: regions of stable liquid phases. Gray area: unstable liquid phases.

in some of the Figures shown above (e.g., see the black continuous lines in Figs. 3 and Fig. 6 at the interface between the LLE and single-liquid phase domains).

Points satisfying $\Psi_r = 0$ at fixed (T_r, P_r) are the solution of Eq. (30) involving 7 dimensionless parameters.

$$\Psi_r\left(\frac{b_2}{b_1}, \frac{a_{c2}}{a_{c1}}, \frac{v_2}{v_1}, \frac{A_{12}}{T}, \frac{A_{21}}{T}, \omega_1, \omega_2\right) = 0 \tag{30}$$

To understand how the regions of stable and unstable liquid phases move with respect to the parameter values, it is proposed to simplify Eq. (30) by proceeding as follows:

- Assumption 1: having empirically observed that the values of the acentric factors little influence the solution of Eq. (30), we propose to fix them to $\omega_1 = \omega_2 = 0.5$.
- Assumption 2: the binary interaction parameters are assumed to be equal: $\frac{A_{12}}{T} = \frac{A_{21}}{T}$. From now on, this dimensionless quantity is denoted A/T. To understand the consequence of this choice, let us look at Fig. 3: imposing $\frac{A_{12}}{T} = \frac{A_{21}}{T}$ is equivalent to reducing the 2-dimensional representation in Fig. 3 to a one-dimensional representation of the information along the first bisector. As a general result, we observed that this first bisector always crosses both regions of single liquid phase and LLE regions when LLE exist. Therefore, we assume that if there exists parameters sets $\left(\frac{A_{12}}{T}, \frac{A_{21}}{T}\right)$ leading to LLE, there will always be possible to find among them some parameter sets obeying the constraint $\frac{A_{12}}{T} = \frac{A_{21}}{T}$.

Finally, Eq. (30) can be condensed as a relation between 4 parameters (see Eq. (31)).

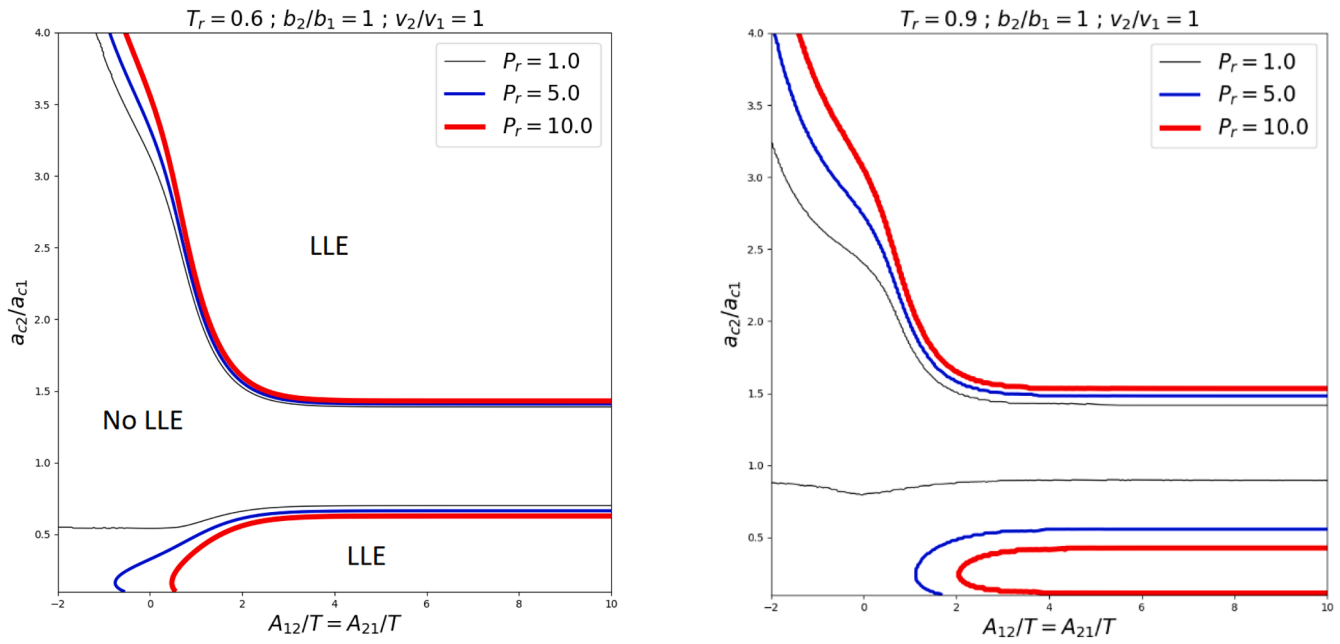

Fig. 7. Contours of the equation $\Psi_r = 0$ in the parameter space $\left(\frac{a_{c2}}{a_{c1}}, \frac{A}{T}\right)$ plotted for $\frac{b_2}{b_1} = 1$ and $\frac{v_2}{v_1} = 1$, calculated with the PR-HV-Wilson EoS. Left panel: the curves are plotted at $\boldsymbol{T_r} = 0.6$ and for $\boldsymbol{P_r} = 1$, **5, 10**. Right panel: the curves are plotted at $\boldsymbol{T_r} = 0.9$ and for $\boldsymbol{P_r} = 1$, **5, 10**. Note that these figures are general (nonspecific to a given mixture) and can be applied to any system characterized by the dimensionless parameters $(\boldsymbol{T_r}, \boldsymbol{b_2}/\boldsymbol{b_1}, \boldsymbol{v_2}/\boldsymbol{v_1})$ indicated above each panel.

$$\begin{cases} (T_r, P_r) \text{ specified} \\ \text{Assumptions}: \ \omega_1 = \omega_2 = 0.5; \ \dfrac{A_{12}}{T} = \dfrac{A_{21}}{T} := \dfrac{A}{T} \\ \Psi_r\left(\dfrac{b_2}{b_1}, \dfrac{a_{c2}}{a_{c1}}, \dfrac{v_2}{v_1}, \dfrac{A}{T}\right) = 0 \end{cases} \tag{31}$$

A base case is now defined: following the spirit of the study carried out by Van Konynenburg and Scott [36,37] to establish a classification of the phase behaviours of binary systems, we consider as reference case the binary systems formed from molecules showing similar sizes and shapes, i.e., that have the same covolumes ($\frac{b_2}{b_1} = 1$) and molar volumes at 298.15 K ($\frac{v_1}{v_2} = 1$).

In such a case, the contours of the equation $\Psi_r = 0$ at a specified (T_r, P_r) can be plotted in the parameter space $\left(\frac{a_{c2}}{a_{c1}}, \frac{A}{T}\right)$, as illustrated in Fig. 7. At a given (T_r, P_r), the LLE regions are delimited by the contours of the equation $\Psi_r = 0$ and are found at the top right and bottom right of each panel.

Two different reduced temperatures (0.6 and 0.9) and three different reduced pressures (1, 5, 10) were considered. These values were selected from the observation of the classification of global phase equilibrium diagrams proposed by Van Konynenburg and Scott which was previously mentioned. In this classification, liquid-liquid phase separation is found in systems of types II to VI. Among these, types II and III, which are by far, the most frequent, report LLE regions at low temperatures ($T < \min\{T_{c1}, T_{c2}\}$) and high pressures only. LLE can be found accidentally at higher temperatures (at $T > T_{c1}$) in diagrams of types IV and V but this type of behaviour should be considered as rare and anecdotal. This justifies why we focused on reduced temperature $T_r = T/T_{c1}$ below 1 and high pressures $P_r = P/P_{c1}$ above 1.

Fig. 7 shows that a LLE region exists for high values of A/T and for low and high values of a_{c2}/a_{c1}. It is noticeable that in the region around $\frac{a_{c2}}{a_{c1}} \approx 1$, the PR-HV-Wilson EoS cannot predict LLE, regardless of the A/T value.

Let us remark that Eq. (31) is symmetric with respect to indices "1" and "2" but is not invariant when these indices are permuted. In other words, if Eq. (31) is solved for given $\left(\frac{b_2}{b_1}, \frac{v_2}{v_1}, \frac{A}{T}\right)$, the solution obtained $\frac{a_{c2}}{a_{c1}}$ will be the reciprocal of the solution found if Eq. (31) is solved for $\left(\frac{b_1}{b_2}, \frac{v_1}{v_2}, \frac{A}{T}\right)$. Both these solutions are thus different while they are actually equivalent and describe the same situation. To eliminate the presence of equivalent solutions in the representations such as the one used in Fig. 7, a convention must be adopted.

It is now recalled that parameters a_c and b of a pure component described by a cubic EoS are $a_c = \Omega_a R^2 T_c^2/P_c$ and $b = \Omega_b RT_c/P_c$, where Ω_a and Ω_b are two universal constants. As a consequence, the ratios b_2/b_1 and a_{c2}/a_{c1} can be expressed with respect to the properties T_c and P_c of both components of the binary system considered:

$$\begin{cases} \dfrac{b_2}{b_1} = \dfrac{T_{c2}}{T_{c1}} \dfrac{P_{c1}}{P_{c2}} \\ \dfrac{a_{c2}}{a_{c1}} = \left(\dfrac{T_{c2}}{T_{c1}}\right)^2 \dfrac{P_{c1}}{P_{c2}} \end{cases} \tag{32}$$

By combining the two expressions of Eq. (32), it is shown that:

$$\frac{a_{c2}}{a_{c1}} = \frac{T_{c2}}{T_{c1}} \frac{b_2}{b_1} \tag{33}$$

The numbering of the components of a binary system is always arbitrary. As a general convention, component 1 is often chosen as the one having the lowest critical temperature: $T_{c1} \leq T_{c2}$.

If this convention is adopted, it follows that $\frac{T_{c2}}{T_{c1}} \geq 1$ and from Eq. (33), one gets: $\frac{a_{c2}}{a_{c1}} \geq \frac{b_2}{b_1}$. Since Fig. 7 was plotted for $\frac{b_2}{b_1} = 1$, this means that only the range $\frac{a_{c2}}{a_{c1}} \geq 1$ should be considered.

The same type of curves as those shown in Fig. 7 were calculated for

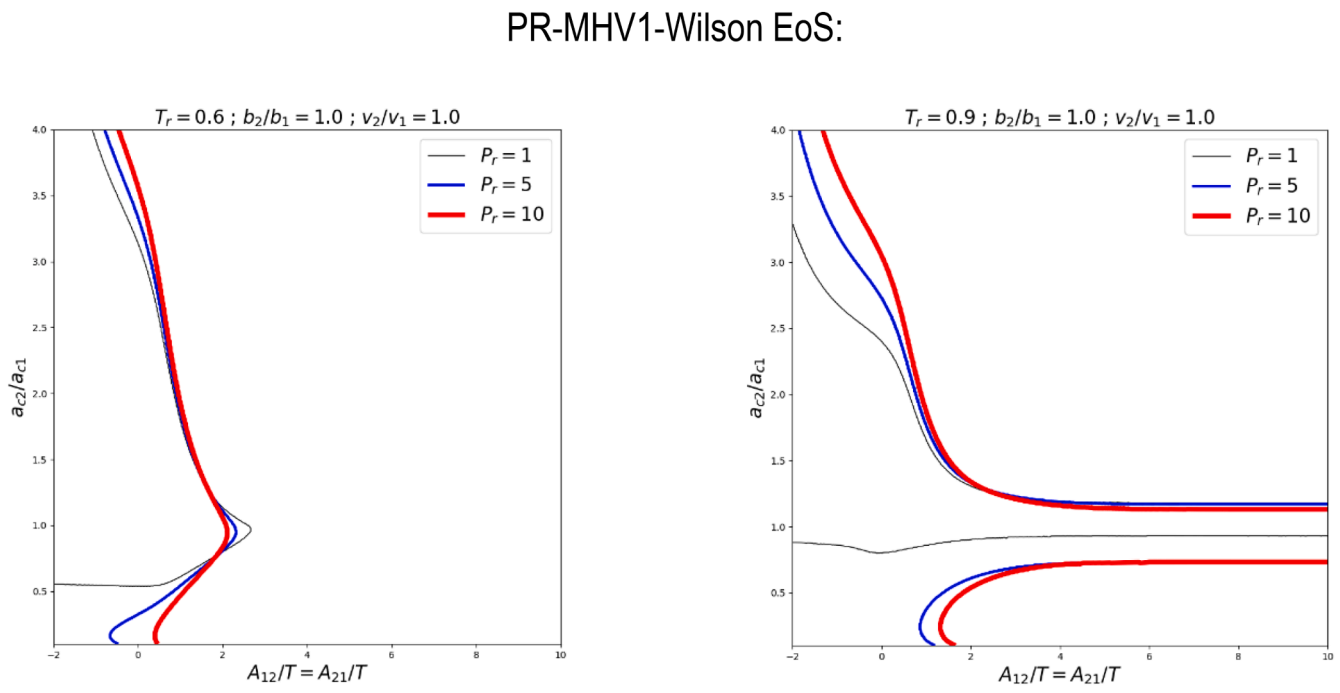

Fig. 8. Contours of the equation $\Psi_r = 0$ in the parameter space $\left(\frac{a_{c2}}{a_{c1}}, \frac{A}{T}\right)$ plotted for $\frac{b_2}{b_1} = 1$ and $\frac{v_2}{v_1} = 1$, calculated with the PR-MHV1-Wilson EoS. See caption of Fig. 7.

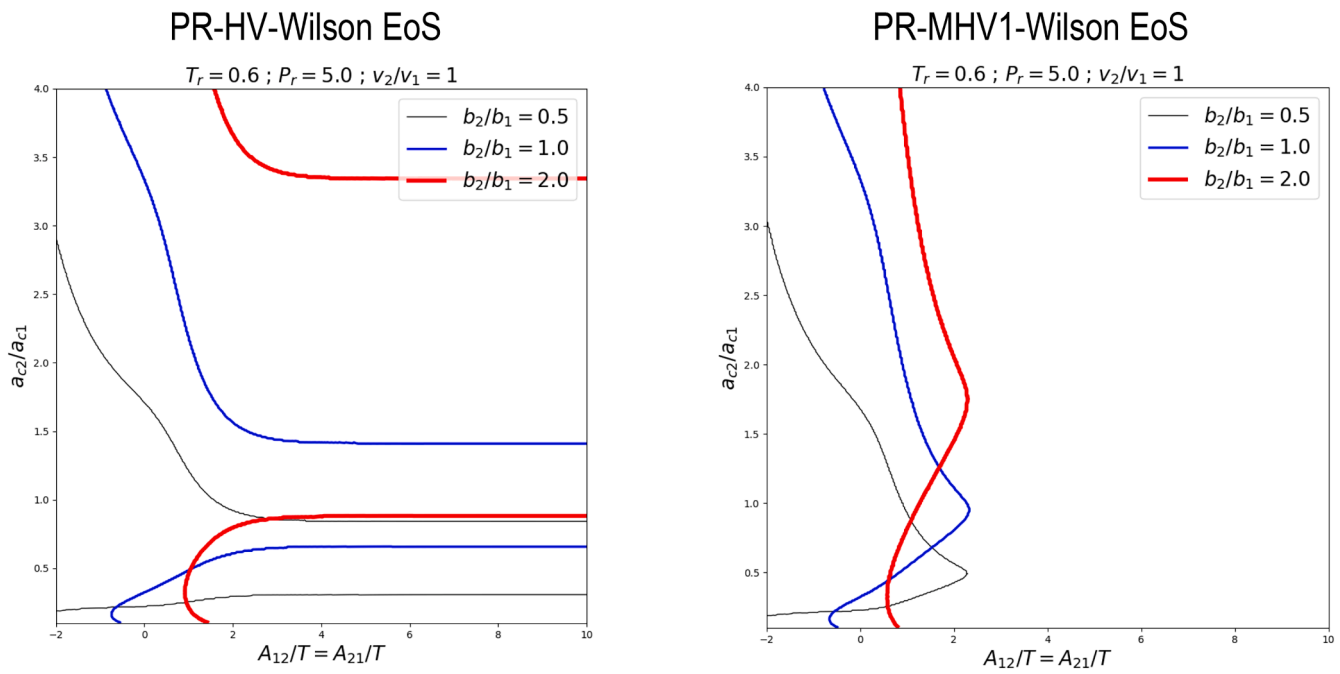

Fig. 9. Contours of the equation $\Psi_r = 0$ in the parameter space $\left(\frac{a_{c2}}{a_{c1}}, \frac{A}{T}\right)$ plotted for $T_r = 0.6$, $P_r = 5$, $b_2/b_1 = 1$ and various values of b_2/b_1, calculated with the PR-HV-Wilson EoS (left panel) and PR-MHV1-Wilson EoS (right panel).

the PR-MHV1-Wilson EoS (in the same conditions as previous, i.e., $\frac{b_2}{b_1} = 1$ and $\frac{v_2}{v_1} = 1$). They are shown in Fig. 8. As mentioned above, if the convention $T_{c2} \geq T_{c1}$ is assumed, only the region associated with $\frac{a_{c2}}{a_{c1}} \geq 1$ should be considered.

At low T_r and high A/T, a LLE region is always obtained regardless of the a_{c2}/a_{c1} value (see the left panel). In other words, at low temperatures, it is always possible to find A/T values so that the EoS PR-MHV1-Wilson model predicts LLE, whereas for the EoS PR-HV-Wilson, we observed that LLE could be predicted if the ratio a_{c2}/a_{c1} was, in addition, sufficiently far from 1.

Regarding the effect of the reduced pressure, it can be concluded that its influence on the size of the LLE regions is modest at low temperature and increases with T_r.

To evaluate how parameters b_2/b_1 and v_2/v_1 influence the LLE prediction, we decided to specify $T_r = 0.6$ and $P_r = 5$ and to plot the contours of $\Psi_r = 0$ in the $\left(\frac{a_{c2}}{a_{c1}}, \frac{A}{T}\right)$ space for different values of b_2/b_1 and v_2/v_1.

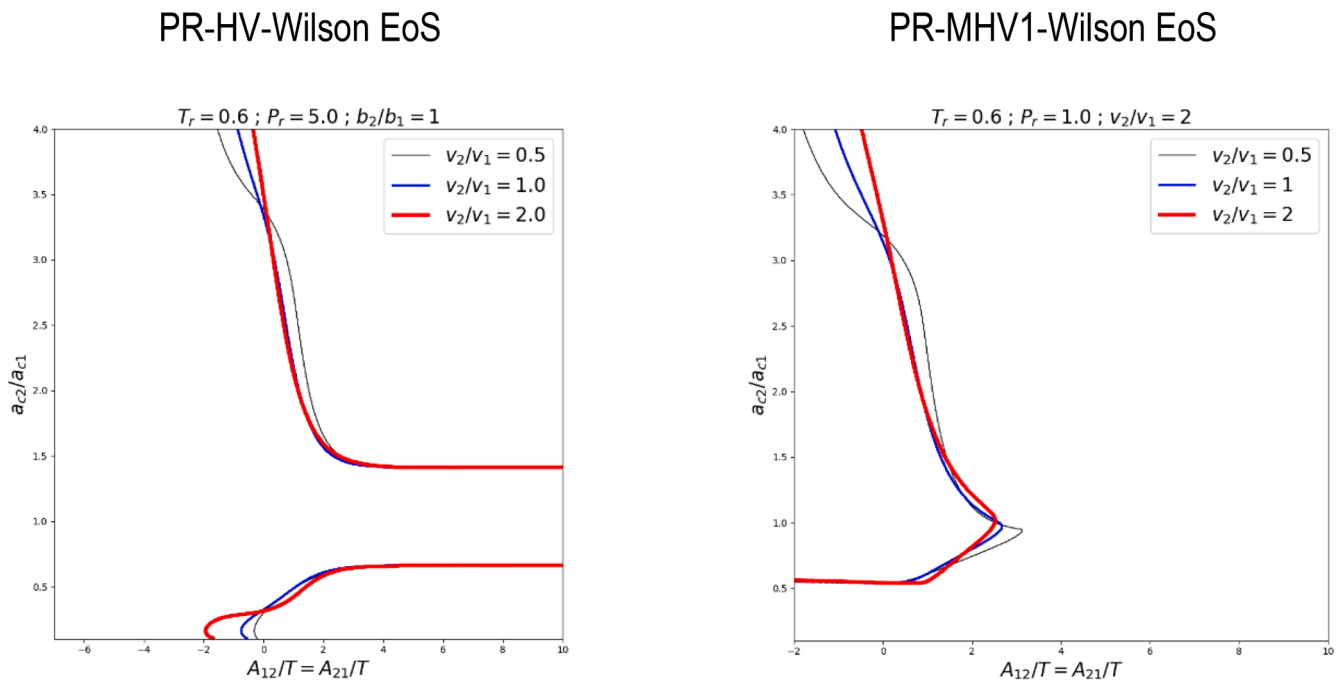

Fig. 10. Contours of the equation $\boldsymbol{\Psi_r} = 0$ in the parameter space $\left(\frac{a_{c2}}{a_{c1}}, \frac{A}{T}\right)$ plotted for $\boldsymbol{T_r} = 0.6$, $\boldsymbol{P_r} = 5$, $\boldsymbol{b_2/b_1} = 1$ and various values of $\boldsymbol{v_2/v_1}$, calculated with the PR-HV-Wilson EoS (left panel) and PR-MHV1-Wilson EoS (right panel).

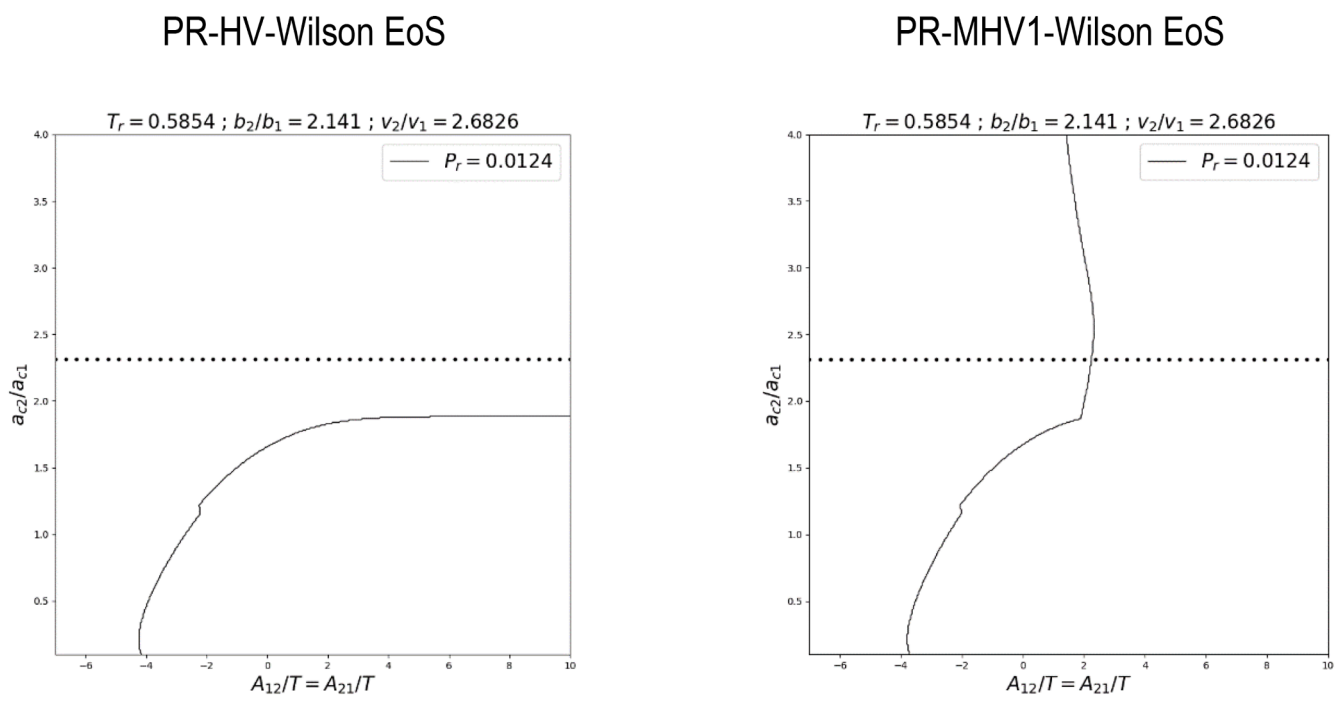

Fig. 11. Contours of the equation $\boldsymbol{\Psi_r} = 0$ in the parameter space $\left(\frac{a_{c2}}{a_{c1}}, \frac{A}{T}\right)$ for the methanol + cyclohexane system in the conditions reported in Fig. 6, i.e., $\boldsymbol{T} = 300$ $\boldsymbol{K}$ ($\boldsymbol{T_r} = 0.585$), $\boldsymbol{P} = 0.1$ $\boldsymbol{MPa}$ ($\boldsymbol{P_r} = 0.0124$), $\boldsymbol{b_2/b_1} = 2.141$, $\boldsymbol{v_2/v_1} = 2.68$ and $\boldsymbol{a_{c2}/a_{c1}} = 2.314$ (dotted line) calculated with the PR-HV-Wilson EoS (left panel) and PR-MHV1-Wilson EoS (right panel).

Figs. 9 and Fig. 10 enable to observe how parameters b_2/b_1 and v_2/v_1, respectively, influence the LLE regions for both the PR-HV-Wilson and PR-MHV1-Wilson EoS. Remembering that only the ranges $\frac{a_{c2}}{a_{c1}} > \frac{b_2}{b_1}$ should be considered, it can concluded that:

- As b_2/b_1 increases (i.e. as the size asymmetry between components 1 and 2 increases), the LLE regions shrink,
- When considering the PR-HV-Wilson model, the ability of the model to predict LLE depends strongly on the value of a_{c2}/a_{c1} and A/T, both of which must be high enough to get liquid instability.

- However, when considering the PR-MHV1-Wilson model, LLE are obtained for high A/T values but for any value of a_{c2}/a_{c1}.
- The prediction of LLE is less sensitive to the parameter v_2/v_1.

To conclude this section, let us go back to the case study of the methanol(1)+cyclohexane(2) system at 300 K and 0.1 MPa. For this system, the ratio a_{c2}/a_{c1} is 2.314, the ratios of covolume b_2/b_1 is 2.141 and the ratio of molar volumes v_2/v_1 at 298.15 K is 2.68. In such conditions, the contours of the equation $\Psi_r = 0$ are reported in Fig. 11. Regardless of the value of A/T, it is never possible for the PR-HV-Wilson EoS to predict LLE at $\frac{a_{c2}}{a_{c1}} = 2.314$. On the contrary, under such conditions, the PR-MHV1-Wilson EoS can predict LLE at high A/T values.

Finally, we would like to draw the reader's attention to the fact that our observations and conclusions can be considered as general and do not depend on the formulation of the Wilson model and, in particular, on the temperature-dependent function used to express the binary parameters. In the present case we have used the Wilson binary parameters A_{12} and A_{21}. Whether these parameters are expressed as constant or temperature dependent functions does not change the contours of the Ψ or Ψ_r functions, since their expressions do not include the temperature derivatives of the Wilson model. It can therefore be claimed that Figs. 3 and Fig. 6–11 are independent of the mathematical formulation used for the binary parameters of the Wilson model: In other words, using constant parameters A_{12} and A_{21} or temperature-dependent functions $A_{12}(T)$ and $A_{21}(T)$ will generate the same contours of the Ψ or Ψ_r functions provided the functions and the constant have the same value at the considered temperature value.

6. Conclusion

In this paper, we set out to demonstrate that the belief that an EoS/g^E model incorporating Wilson's full model cannot predict LLEs is incorrect. Of course, at the matching pressure at which the excess Gibbs energies from the EoS and from Wilson's model are equated ($+\infty$ in the HV mixing rule and 0 in the ZRP mixing rule), this statement is obviously true as the Gibbs energy change on mixing predicted from both models are strictly identical. However, at pressure different from the matching pressure, there is no reason to claim that the EoS/g^E model cannot predict LLE.

In particular, we have shown that with the PR-HV-Wilson, the occurrence of LLE increases when (i) the covolumes b_1 and b_2 are similar, when (ii) the critical attractive parameters satisfy $a_{c2} \gg a_{c1}$ and when (iii) $\frac{A}{T}$ values are high enough. In terms of critical temperature and pressure, these conditions can be written as: $T_{c2} \gg T_{c1}$ and $\frac{P_{c2}}{P_{c1}} \approx \frac{1}{T_{c2}/P_{c1}}$. This trend is classically observed when a light compound is mixed with a heavy compound.

It was observed that the prediction of LLE from the PR-MHV1-model is easier and requires fewer conditions. In particular, it was found that this model is less sensitive to the condition of similar covolume (LLE were observed for all the values of b_2/b_1 considered, including values far from 1).

We conclude this article by stating that there is definitely no reason to rule out the Wilson model from incorporation into a cubic EoS via an EoS/g^E approach. Wilson's model has all the features one would expect from an activity coefficient model and, when combined with an EoS, the resulting model can predict LLE.

CRediT authorship contribution statement

Romain Privat: Writing – original draft, Software, Methodology, Investigation, Conceptualization. **Jean-Noël Jaubert:** Writing – original draft, Methodology, Investigation, Conceptualization. **Georgios M. Kontogeorgis:** Writing – original draft, Methodology, Investigation, Conceptualization.

Declaration of competing interest

The authors declare that they have no known competing financial interests or personal relationships that could have appeared to influence the work reported in this paper.

Appendix 1. Detailed analysis of the combinatorial and residual contributions to $g^{E,EoS}$ for two systems modelled with the PR-HV-Wilson and the PR-MHV1-Wilson EoS

In this section, we go deeper into the comparison started in Sections 4.3 and 4.4, between the $g^{E,EoS}$ predicted from the EoS and the $g^{E,\gamma}$ obtained from the Wilson AC model. The comparison of the separate residual and combinatorial contributions is proposed here.

Two cases are considered here:

- The system ethane + toluene at 280 K and 3 MPa, modelled with the PR-HV-Wilson model (introduced in Section 4.3),
- The system methanol + cyclohexane at 300 K and 0.1 MPa, modelled with the PR-MHV1-Wilson model (introduced in Section 4.4).

For both of them, the binary interaction parameters are set to: $A_{12} = A_{21} = 1000$ K. These values were selected in order to produce LLE in the temperature and pressure conditions considered.

Let us observe, in Figs. 12 and Fig. 13, how the different terms (residual, combinatorial and $\frac{Pv^E}{RT}$), present in the g^E functions of the AC model and CEoS, behave. The relationship between these different contributions is recalled in Eq. (34).

$$\begin{cases} \dfrac{g^{E,EoS}}{RT} = \dfrac{a^{E,EoS}_{comb}}{RT} + \dfrac{a^{E,EoS}_{res}}{RT} + \dfrac{Pv^{E,EoS}}{RT} \\ \dfrac{g^{E,\gamma}}{RT} = \dfrac{a^{E,\gamma}_{comb}}{RT} + \dfrac{a^{E,\gamma}_{res}}{RT} + 0 \end{cases} \tag{34}$$

The first noticeable difference between the AC and EoS models lies in the $\frac{Pv^E}{RT}$: the $\frac{Pv^{E,\gamma}}{RT}$ term of Wilson is zero because AC model are pressure independent and $v^{E,\gamma}$ is the pressure derivative of $g^{E,\gamma}$, while the $\frac{Pv^{E,EoS}}{RT}$ is not. Note that due to the nullity of $v^{E,\gamma}$, $g^{E,\gamma}$ and $a^{E,\gamma}$ are strictly equal. However, Fig. 12 (ethane + toluene system, PR-HV-Wilson model) Fig. 13 (methanol + cyclohexane system, PR-MHV1-Wilson model) show that the $\frac{Pv^{E,EoS}}{RT}$ contribution is small (much lower than those of the other contributions). Therefore, the $\frac{Pv^{E,EoS}}{RT}$ term has little effect on the $\frac{g^{E,EoS}}{RT}$ and $\frac{g^{M,EoS}}{RT}$ values (this statement is confirmed by the plotting of the function $\left(\frac{g^{M,EoS}}{RT} - \frac{Pv^{E,EoS}}{RT}\right)$ – not reported here – which has the same features as the $\frac{g^{M,EoS}}{RT}$ function).

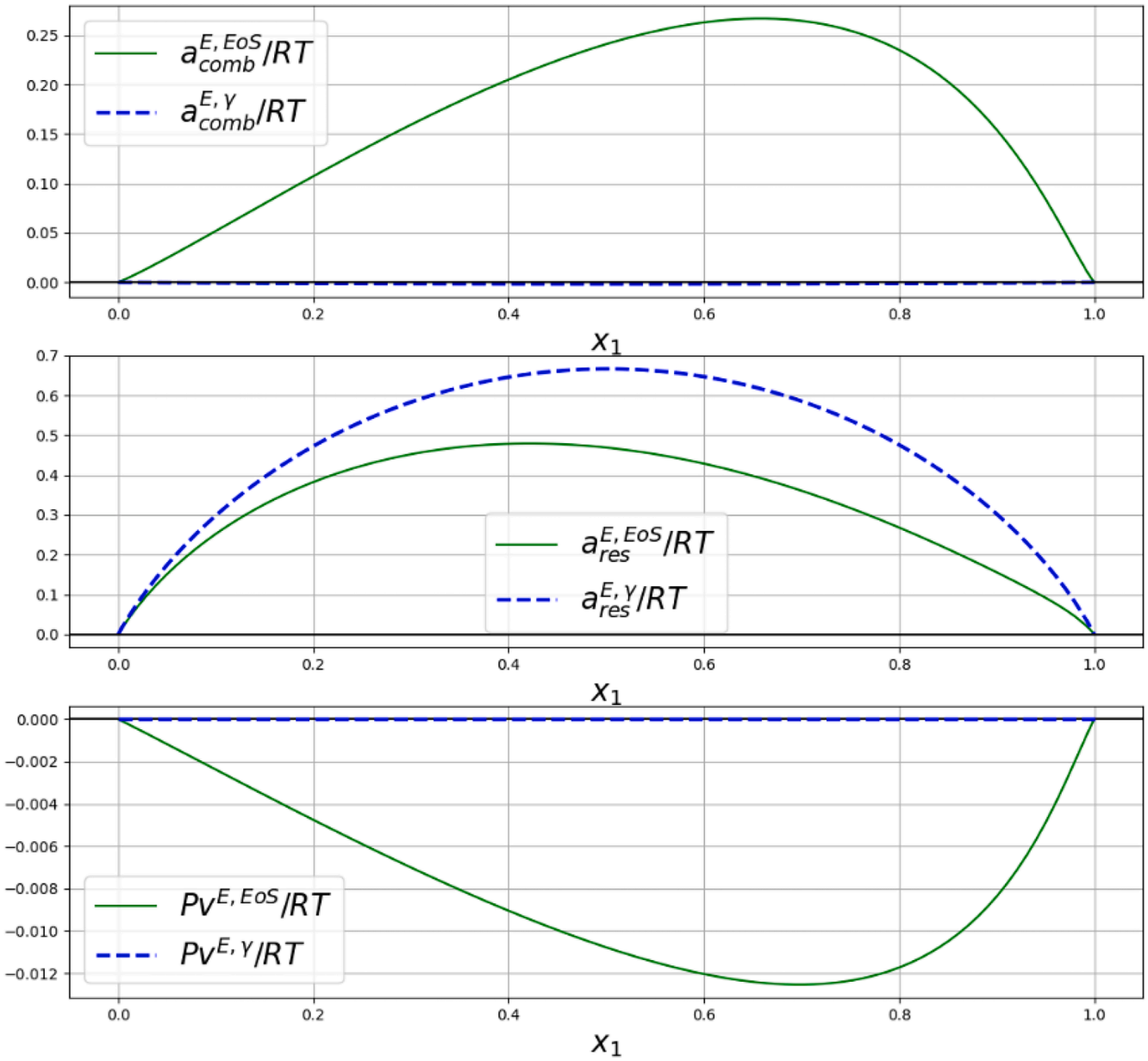

Fig. 12. System ethane(1) + toluene(2) at 280 K and 3 MPa. Representation of the three contributions to the $g^E/(RT)$ function: combinatorial, residual and $Pv^E/(RT)$. Continuous lines: PR-HV-Wilson model, dashed lines: complete Wilson AC model (γ).

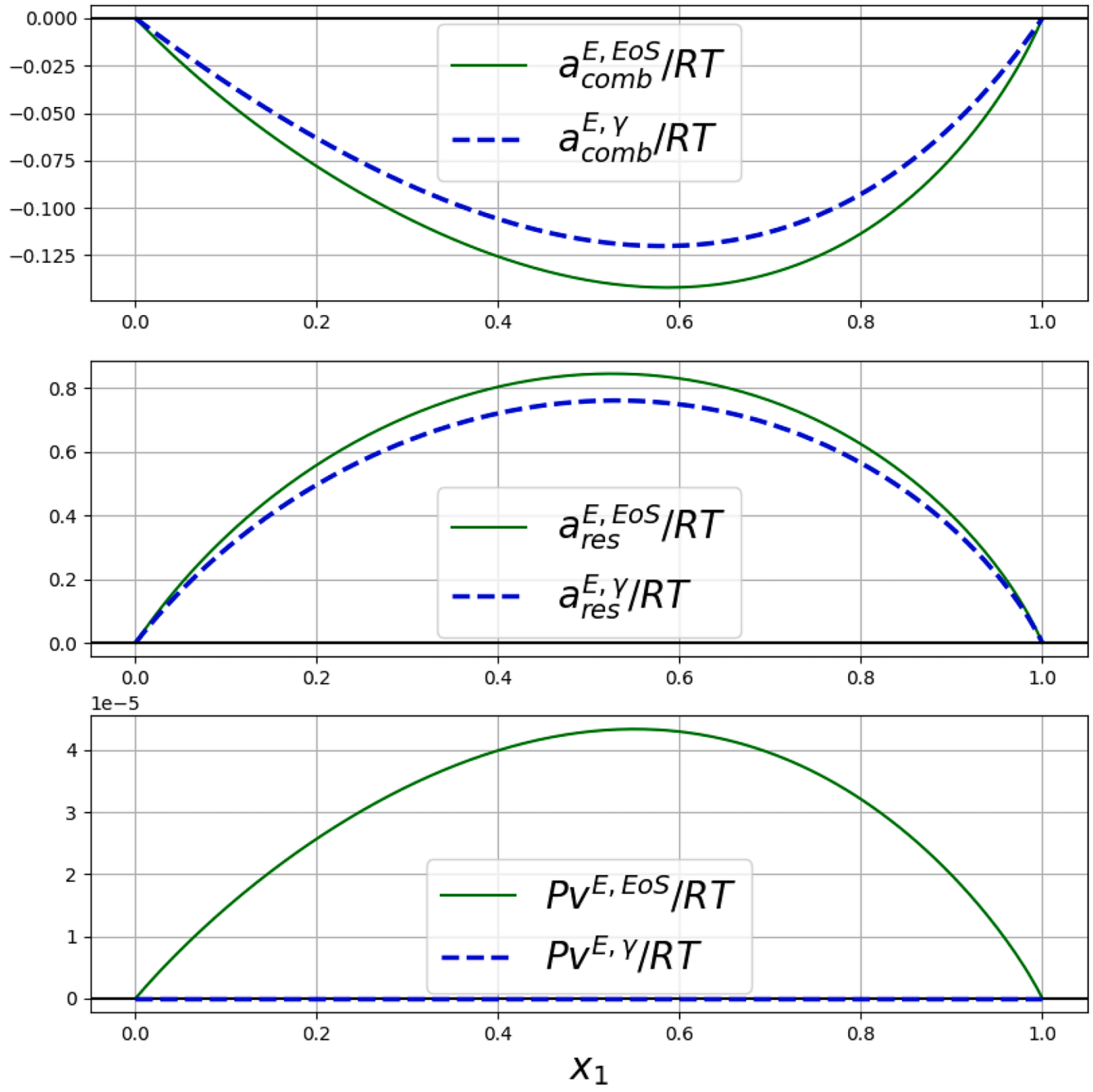

Fig. 13. System methanol(1) + cyclohexane(2) at 300 K and 0.1 MPa. Representation of the three contributions to the $\boldsymbol{g^E/(RT)}$ function: combinatorial, residual and $\boldsymbol{Pv^E/(RT)}$. Continuous lines: PR-MHV1-Wilson model, dashed lines: complete Wilson AC model (γ).

The residual and combinatorial contributions play an important role in the generation of liquid instability and the specific responsibility of each in the final effect is difficult to identify separately. Their expressions are recalled in Eq. (22) (with $k = 0$, for the HV mixing rule). It can be observed that:

- As previously discussed, the combinatorial terms of the CEoS and AC models have very different functional forms and dependencies on the composition variable.
- The residual term of the CEoS is a complex function of the Wilson AC model involving not only $\frac{g^{E,\gamma}(T,\boldsymbol{x})}{RT}$, but also the volumes v and covolume b of the mixture which both depend on $\boldsymbol{x}$ and therefore, influence the liquid instability criterion.

The different expressions used for the combinatorial terms of the CEoS and Wilson AC models can explain the very different values of these terms for the binary system ethane + toluene at given (T, P) shown in Fig. 12: the combinatorial term of the AC model involves molar volumes (volume v_i of the pure species at 298.15 K and volume v of the mixture) that are all of similar magnitude, resulting in a small value of $\frac{a_{comb}^{E,\gamma}}{RT}$ -(the maximum absolute value is around $2{\cdot}10^{-3}$). The combinatorial term of the CEoS, expressed in terms of free volumes, is much higher (maximum absolute value around $3{\cdot}10^{-1}$) because the covolumes and therefore, the free volumes of the compounds are significantly different.

The opposite observations could be made regarding the methanol + cyclohexane system (see Fig. 13). In that case, the combinatorial terms coming

from the EoS and Wilson's model are similar.

Regarding the residual contributions of the AC model and CEoS, they are of similar magnitude in all cases (see Figs. 12 and Fig. 13).

As explained in Section 4.3, the Gibbs energy change on mixing $g^{M,EoS}/(RT)$ is the addition of the EoS excess Gibbs energy $g^{E,EoS}/(RT)$ and the ideal mixing Gibbs energy $g^{M,id}/(RT)$. The isothermal isobaric curves $g^{M,EoS}/(RT)$ versus molar fraction are shown in Fig. 5 (ethane + toluene) and Fig. 14 (methanol + cyclohexane).

In all cases, the properties $g^{E,EoS}/(RT)$ and $g^{M,id}/(RT)$ are of similar magnitude but opposite signs. This results in small values of $g^{M,EoS}/(RT)$ with respect to $g^{E,EoS}/(RT)$ and $g^{M,id}/(RT)$.

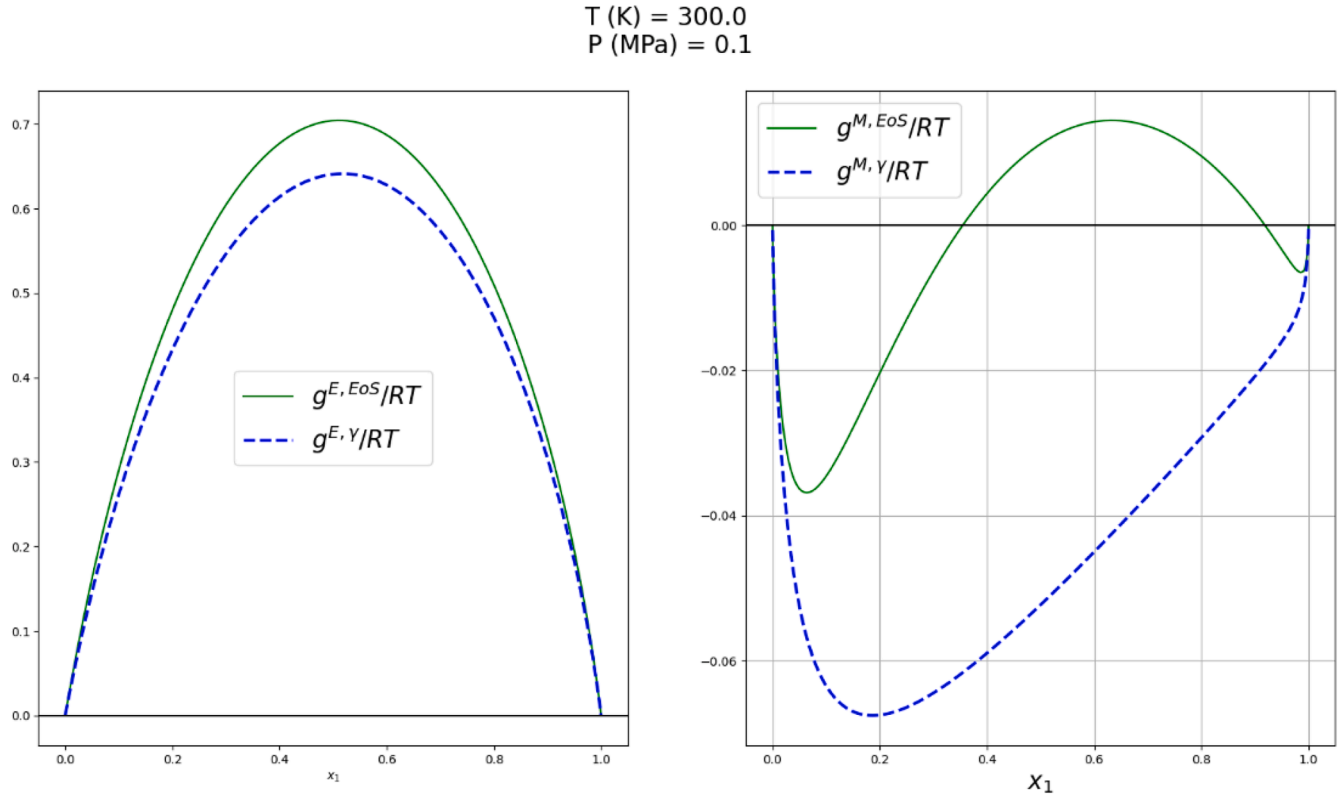

Fig. 14. System methanol(1) + cyclohexane(2) at 300 K and 0.1 MPa. Representation of the g^M/RT and g^E/RT curves modelled with the complete Wilson AC model (γ) and the PR-MHV1-Wilson EoS.

Which lesson should we learn from this study? we need to conclude that the comparison and analysis of the combinatorial and residual contributions coming from the EoS and from Wilson's model is not of great help to understand why some models can model LLE while some others cannot.

In all cases, the $g^{M,EoS}/(RT)$ curve, the curvature of which is the key information for LLE prediction, results from the addition of two terms of similar magnitude ($g^{E,EoS}/(RT)$ and $g^{M,id}/(RT)$), one positive, the other negative. It seems quite difficult to identify which contribution to $g^{E,EoS}/(RT)$ is responsible for the final curvature of the function $g^{M,EoS}/(RT)$ versus x_1.

Appendix 2. Modelling of the system ethane + toluene using the PR-HV-NRTL and the PR-MHV1-NRTL EoS

This section attempts to show that the incorporation of Wilson's model into the PR EoS, using either the HV or MHV1 mixing rule, produces a behaviour similar to that of any other model formed in the same way.

The system ethane(1) + toluene(2) modelled with the PR-HV-NRTL and PR-MHV1-NRTL models is used as an illustrative example. The expression of the NRTL activity coefficient model is given in Eq. (35).

$$\frac{g^{E,\gamma}}{RT} = x_1 x_2 \left(\frac{\tau_{21} G_{21}}{x_1 + x_2 G_{21}} + \frac{\tau_{12} G_{12}}{x_2 + x_1 G_{12}} \right) \quad with : \begin{cases} \tau_{12} = \dfrac{A_{12}}{T} \text{and} G_{12} = \exp(-\alpha_{12}\tau_{12}) \\ \tau_{21} = \dfrac{A_{21}}{RT} \text{and} G_{21} = \exp(-\alpha_{12}\tau_{21}) \\ \alpha_{12} = 0.3 \end{cases} \tag{35}$$

The same calculations as those used to generate Fig. 3 were repeated with EoS combined with the NRTL model instead of the Wilson model. The results of these calculations are presented in Fig. 15.

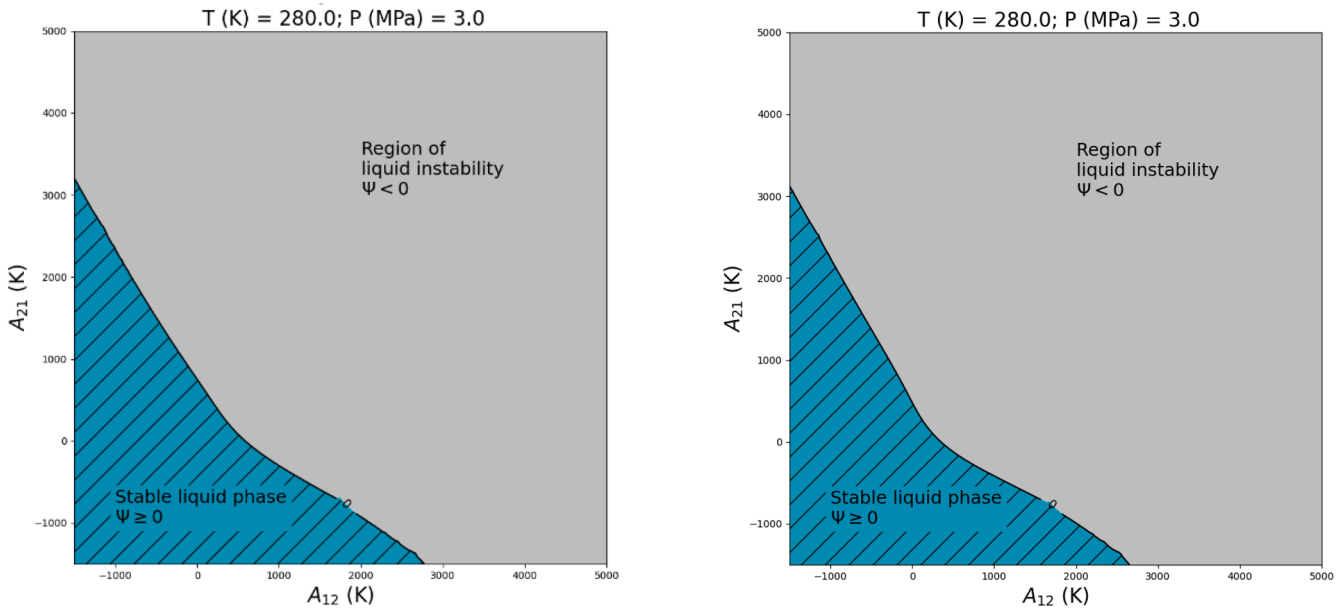

Fig. 15. Sign of the Ψ function, defined by Eq. (11) in the parameter space $(\boldsymbol{A}_{12}, \boldsymbol{A}_{21})$ for the system ethane(1) + toluene(2) at 280 K and 3 MPa modelled with the PR-HV-NRTL model (left side) and the PR-MHV1-NRTL model (right side). Hatched area: regions of stable liquid phases ($\boldsymbol{\Psi} \geq 0$). Non-hatched area: unstable liquid phases ($\boldsymbol{\Psi} < 0$).

Overall, there is not a significant difference of behaviour between Wilson-based models (see Fig. 3) and NRTL-based models (see Fig. 15). In both cases, the region of liquid instability is obtained for high values of A_{12} and A_{21}. Interesting is the similarity of behaviour between the PR-HV-NRTL and PR-MHV1-NRTL models that was not observed between the PR-HV-Wilson and PR-MHV1-Wilson models.

Data availability

No data was used for the research described in the article.

References

[1] M.-J. Huron, J. Vidal, New mixing rules in simple equations of state for representing vapour-liquid equilibria of strongly non-ideal mixtures, Fluid Phase Equilib. 3 (1979) 255–271, https://doi.org/10.1016/0378-3812(79)80001-1.
[2] J. Mollerup, A note on the derivation of mixing rules from excess Gibbs energy models, Fluid Phase Equilib. 25 (1986) 323–327, https://doi.org/10.1016/0378-3812(86)80007-3.
[3] M.L. Michelsen, A modified Huron-Vidal mixing rule for cubic equations of state, Fluid Phase Equilib. 60 (1990) 213–219, https://doi.org/10.1016/0378-3812(90)85053-D.
[4] M.L. Michelsen, A method for incorporating excess Gibbs energy models in equations of state, Fluid Phase Equilib. 60 (1990) 47–58, https://doi.org/10.1016/0378-3812(90)85042-9.
[5] G.M. Kontogeorgis, G.K. Folas, Thermodynamic Models For Industrial Applications, John Wiley & Sons, Ltd, Chichester, UK, 2010, https://doi.org/10.1002/9780470747537.
[6] S. Dahl, A. Fredenslund, P. Rasmussen, The MHV2 model: a UNIFAC-based equation of state model for prediction of gas solubility and vapor-liquid equilibria at low and high pressures, Ind. Eng. Chem. Res. 30 (1991) 1936–1945, https://doi.org/10.1021/ie00056a041.
[7] S. Dahl, M.L. Michelsen, High-pressure vapor-liquid equilibrium with a UNIFAC-based equation of state, AIChE J 36 (1990) 1829–1836, https://doi.org/10.1002/aic.690361207.
[8] V. Feroiu, D. Geană, Prediction of vapor-liquid equilibria at high pressures using activity coefficients at infinite dilution, Fluid Phase Equilib. 120 (1996) 1–10, https://doi.org/10.1016/0378-3812(96)02993-7.
[9] Ch. Lermite, J. Vidal, High pressure polar compounds phase equilibria calculation : mixing rules and excess properties, Fluid Phase Equilib. 42 (1988) 1–19, https://doi.org/10.1016/0378-3812(88)80047-5.
[10] C. Lermite, J. Vidal, A group contribution equation of state for polar and non-polar compounds, Fluid Phase Equilib. 72 (1992) 111–130, https://doi.org/10.1016/0378-3812(92)85021-Y.
[11] G. Soave, Improvement of the Van Der Waals equation of state, Chem. Eng. Sci. 39 (1984) 357–369, https://doi.org/10.1016/0009-2509(84)80034-2.
[12] G. Soave, A new expression of q(α) for the modified Huron-Vidal method, Fluid Phase Equilib. 72 (1992) 325–328, https://doi.org/10.1016/0378-3812(92)85034-6.
[13] G.S. Soave, A. Bertucco, L. Vecchiato, Equation-of-state group contributions from infinite-dilution activity coefficients, Ind. Eng. Chem. Res. 33 (1994) 975–980, https://doi.org/10.1021/ie00028a027.
[14] G.S. Soave, S. Sama, M.I. Oliveras, A new method for the prediction of VLE and thermodynamic properties. Preliminary results with alkane–ether–alkanol systems, Fluid Phase Equilib. 156 (1999) 35–50, https://doi.org/10.1016/S0378-3812(99)00022-9.
[15] J.-N. Jaubert, F. Mutelet, VLE predictions with the Peng-Robinson equation of state and temperature-dependent k_{ij} calculated through a group contribution method, Fluid Phase Equilib. 224 (2004) 285–304, https://doi.org/10.1016/j.fluid.2004.06.059.
[16] J.-N. Jaubert, J.-W. Qian, S. Lasala, R. Privat, The impressive impact of including enthalpy and heat capacity of mixing data when parameterising equations of state. Application to the development of the *E*-PPR78 (Enhanced-Predictive-Peng-Robinson-78) model, Fluid Phase Equilib. 560 (2022) 113456, https://doi.org/10.1016/j.fluid.2022.113456.
[17] R. Privat, J.-N. Jaubert, The state of the art of cubic equations of state with temperature-dependent binary interaction coefficients: from correlation to prediction, Fluid Phase Equilib. 567 (2023) 113697, https://doi.org/10.1016/j.fluid.2022.113697.
[18] J.-W. Qian, R. Privat, J.-N. Jaubert, P. Duchet-Suchaux, Enthalpy and heat capacity changes on mixing: fundamental aspects and prediction by means of the PPR78 cubic equation of state, Energy Fuels 27 (2013) 7150–7178, https://doi.org/10.1021/ef401605c.
[19] T. Holderbaum, J. Gmehling, PSRK: a group contribution equation of state based on UNIFAC, Fluid Phase Equilib. 70 (1991) 251–265, https://doi.org/10.1016/0378-3812(91)85038-V.
[20] S. Horstmann, K. Fischer, J. Gmehling, PSRK group contribution equation of state: revision and extension III, Fluid Phase Equilib. 167 (2000) 173–186, https://doi.org/10.1016/S0378-3812(99)00333-7.
[21] J. Chen, K. Fischer, J. Gmehling, Modification of PSRK mixing rules and results for vapor–liquid equilibria, enthalpy of mixing and activity coefficients at infinite dilution, Fluid Phase Equilib. 200 (2002) 411–429, https://doi.org/10.1016/S0378-3812(02)00048-1.
[22] J. Gmehling, Potential of thermodynamic tools (group contribution methods, factual data banks) for the development of chemical processes, Fluid Phase Equilib. 210 (2003) 161–173, https://doi.org/10.1016/S0378-3812(03)00177-8.
[23] S. Horstmann, A. Jabłoniec, J. Krafczyk, K. Fischer, J. Gmehling, PSRK group contribution equation of state: comprehensive revision and extension IV, including critical constants and α-function parameters for 1000 components, Fluid Phase Equilib. 227 (2005) 157–164, https://doi.org/10.1016/j.fluid.2004.11.002.
[24] R. Privat, J.-N. Jaubert, G.M. Kontogeorgis, The secret of the Wilson equation, Fluid Phase Equilib. 579 (2024) 114018, https://doi.org/10.1016/j.fluid.2023.114018.

[25] Y.Le Guennec, R. Privat, J.-N. Jaubert, Development of the translated-consistent *tc*-PR and *tc*-RK cubic equations of state for a safe and accurate prediction of volumetric, energetic and saturation properties of pure compounds in the sub- and super-critical domains, Fluid Phase Equilib. 429 (2016) 301–312, https://doi.org/10.1016/j.fluid.2016.09.003.

[26] Y.Le Guennec, S. Lasala, R. Privat, J.-N. Jaubert, A consistency test for α-functions of cubic equations of state, Fluid Phase Equilib. 427 (2016) 513–538, https://doi.org/10.1016/j.fluid.2016.07.026.

[27] Y.Le Guennec, R. Privat, S. Lasala, J.-N. Jaubert, On the imperative need to use a consistent α-function for the prediction of pure-compound supercritical properties with a cubic equation of state, Fluid Phase Equilib. 445 (2017) 45–53, https://doi.org/10.1016/j.fluid.2017.04.015.

[28] A. Pina-Martinez, R. Privat, I.K. Nikolaidis, I.G. Economou, J.-N. Jaubert, What is the optimal activity coefficient model to be combined with the *translated–consistent* Peng–Robinson equation of state through advanced mixing rules? Cross-comparison and grading of the Wilson, UNIQUAC, and NRTL a^E models against a benchmark database involving 200 binary systems, Ind. Eng. Chem. Res. 60 (2021) 17228–17247, https://doi.org/10.1021/acs.iecr.1c03003.

[29] J.-N. Jaubert, R. Privat, Y.Le Guennec, L. Coniglio, Note on the properties altered by application of a Péneloux–type volume translation to an equation of state, Fluid Phase Equilib. 419 (2016) 88–95, https://doi.org/10.1016/j.fluid.2016.03.012.

[30] R. Privat, J.-N. Jaubert, Y.Le Guennec, Incorporation of a volume translation in an equation of state for fluid mixtures: which combining rule? Which effect on properties of mixing? Fluid Phase Equilib. 427 (2016) 414–420, https://doi.org/10.1016/j.fluid.2016.07.035.

[31] J.M. Smith, H.C. Van Ness, M.M. Abbott, Introduction to Chemical Engineering Thermodynamics, 7th ed, McGraw-Hill, Boston, 2005.

[32] M.L. Michelsen, J.M. Mollerup, Thermodynamic models: Fundamentals & Computational Aspects, 2. ed, Tie-Line Publications, Holte, 2007.

[33] DIPPR's Project 801 Database, DIPPR: design Institute for Physical Properties (n. d.). https://www.aiche.org/dippr. 2024.

[34] J.-N. Jaubert, R. Privat, Application of the double-tangent construction of coexisting phases to any type of phase equilibrium for binary systems modeled with the gamma-phi approach, Chem. Eng. Educ. 48 (2014) 42–56.

[35] H. Renon, J.M. Prausnitz, Local compositions in thermodynamic excess functions for liquid mixtures, AIChE J 14 (1968) 135–144, https://doi.org/10.1002/aic.690140124.

[36] P.H. Van Konynenburg, R.L. Scott, Critical Lines and Phase Equilibria in Binary Van Der Waals Mixtures, Philos. Trans. R. Soc., A 298 (1980) 495–540, https://doi.org/10.1098/rsta.1980.0266.

[37] R. Privat, J.-N. Jaubert, Classification of global fluid-phase equilibrium behaviors in binary systems, Chem. Eng. Res. Des. 91 (2013) 1807–1839, https://doi.org/10.1016/j.cherd.2013.06.026.